MECHANISMS AND PROCESSES OF SUSPENDED SEDIMENT TRANSPORT AND DEPOSITION IN HIGH ARCTIC PROGLACIAL LAKE LINNÉVATNET, SPITSBERGEN, SVALBARD

by

S. Benjamin B. Schupack

A thesis submitted in partial fulfillment of the requirements for graduation with Honors in Department of Geology and Department of Environmental Studies

Whitman College
2007

Table of Contents

List of Figures……..3
Abstract……6
1. Introduction...……..7
1.1. Purpose…….……...7
1.2. Justification: Climate Change……...……...7
1.3. Site Description……9
1.3.1. Linnédalen……...11
1.4. Tectonic Background of Linnédalen…….....13
1.4.1. Bedrock of Linnédalen……....14
1.5. Components of Linnédalen..……..16
1.5.1 Glacier Linnébreen…...……....16
1.5.2. River Linnéelva…….……17
1.5.3. Lake Linnévatnet..…...……...18
1.6. Sediments in Linnévatnet…….....20
1.7. Discharge and Suspended Sediment…..…….....21
1.8. Hydroclimate: Stratification & Currents……23
1.8.1. Lacustrine Stratification…...……...…23
1.8.2. Currents…….....…….…..16
2. Methods……..……...…28
2.1. Fieldwork……..…….....28
2.2. Meteorological Station…….…….……28
2.3. Temperature Data-loggers……...….30
2.4. Water Column Profiles…… …….....31
2.5. Automated Imaging……...……34
2.6. Simultaneous Adjacent Projects……....35
3. Results……..…...……..36
3.1. Weather Station..…...……..…36
3.1.1. Air Temperature……..…36
3.1.2. Wind Velocity and Wind Direction……....36
3.1.3. Precipitation……..…….....37

3.1.4. Solar Radiation……..……..38
3.1.5. Soil Temperatures……...39
3.2. Lake Temperature ……....40
3.2.1. Lake Temperature and Meteorological Conditions……44
3.3. Water Column Profiles……..47
3.4. Correlating Lake Density Currents and Meteorological Conditions…….…54
3.5. Water Temperature and Density Currents…….58
3.6. Correlating Lake Inlet Currents and Suspended Sediment Concentration…60
3.7. Automated Remote Imaging……..62
4. Discussion…..……...69
4.1. Discharge and Suspended Sediment Concentration ……..69
4.2. Linnévatnet Density Currents……69
4.3. Lake Temperatures……73
4.4. Paleoclimatic Significance…….……74
4.5. Other Sources of Sediment Input…….……..76
4.6. Field Season Logistics and early Summer Melt……77
5. Conclusions……...……78
5.1. Future Work…...……79
Acknowledgments. ……80
Literature Cited.……81

List of Figures

Figure 1. Global view of Svalbard and study site Kapp Linné…….……11
Figure 2. Satellite image of Linnédalen Valley……12
Figure 3. The geology of Linnédalen……..5
Figure 4. Oblique aerial photographs of the Linnébreen glacier in the Linné valley in 1936 and 1995……...…….17
Figure 5. Bathymetry of Linnévatnet with superimposed position of each mooring location and camera placement……..19
Figure 6. Isopach map of sediments in Linnévatnet…….20
Figure 7. Suspended sediment hysteresis……..22
Figure 8. Sketch of inflow mixing patterns in glacier-fed lakes……...25
Figure 9. Sketch of homopycnal inflow mixing in meltwater lakes…….26
Figure 10. Automated weather station 500 m south of Lake Linné records meteorological conditions at 30-minute resolution. ……...……29
Figure 11. Water column profiles of depth and % light transmission were measured with the Seabird Instruments® Seacat® SBE 19 Profiler…..……..32
Figure 12. Vertical casts involved lowering the Seacat® into the water column at mooring sites throughout the lake……....32
Figure 13. Mooring sites at the southern end of Linnévatnet……...33
Figure 14. Programming the solar-powered automated camera to capture an image of the lake inlet every three hours……34
Figure 15. Air temperature in Linnédalen between 18 July 2006 and 15 August 2006...36
Figure 16. Rainfall in Linnédalen between 18 July and 15 August 2006..……...…37
Figure 17. Solar radiation in Linnédalen between 18 July and 15 August 2006……..38
Figure 18. Soil temperatures from 18 July to 15 August 2006 at 0.5 m and 1.5 m below the surface..……39
Figure 19. Soil temperature at 0.5 m and 1.5 m from 14 January 06 to 15 August 06….40
Figure 20. Linnévatnet temperatures from 11 August 2005 to 10 August 2006……..…41
Figure 21. Water temperatures at mooring C from 18 July to 10 August 2006, at depths of 2.5 m, 5.5 m, 9.5 m, 13.5 m, and the bottom sediment at 15.2 m…....……..42

Figure 22. Water temperatures at mooring D from 18 July to 10 August 2006, at depths of 2 m, 9 m, and 13 m……..…….42
Figure 23. Water temperatures at mooring E from 18 July to 10 August 2006, at depths of 3 m, 4 m, and 5 m……..43
Figure 24. Water temperatures at mooring F from 18 July to 9 August 2006, at depths of 3 m, 6 m, 9 m, and the lake floor at 10 m. ……43
Figure 25. Water temperatures at mooring G from 18 July to 10 August 2006, at depths of 10 m, 20 m, 30 m, and 35 m……..44
Figure 26. Wind direction and mooring C water temperatures from 18 July to 10 August 2006……....45
Figure 27. Wind speed and mooring C water temperatures from 18 July to 10 August 2006……....45
Figure 28. Air temperature and mooring C water temperatures from 18 July to 10 August 2006…….……...…46
Figure 29. Precipitation and mooring C lake temperatures from 18 July to 10 August 2006…….……...46
Figure 30. Solar radiation and mooring C lake temperatures from 18 July to 10 August 2006…….……...47
Figure 31. Vertical transmissivity profile for an overflow current at Mooring C…….…48
Figure 32. An underflow current half way between the east shore and the red boat…….49
Figure 33. The transmissivities from the red boat and half way between the red boat and mooring C reveal the termination of an overflow and beginning of an underflow current……50
Figure 34. The transmissivity profile of the only interflow detected within Linnévatnet……51
Figure 35. Great increases in turbidity in the bottom meter of the water column probably are the result of delta turbidity currents…….52
Figure 36. Homopycnal currents in Linnévatnet as a result of mixing from wind and wave action……....53
Figure 37. The influence of meteorological factors on lake inlet transmissivities at different depths from 17 July to 16 August 2006…..…….…56

Figure 38. The influence of meteorological factors on mooring C transmissivities at different depths from 17 July to 16 August 2006……..…57
Figure 39. An apparent correlation between lake temperature and transmissivity…..….58
Figure 40. Variation in lake temperature, but no variation in transmissivity……59
Figure 41. Little variation in temperature, but great variation in transmisivity…….60
Figure 42. Suspended sediment concentration (SSC) and discharge (Q) of Linnéelva from 17 July to 16 August 2006……..……...61
Figure 43. Discharge (Q) and suspended sediment concentration (SSC) compared with inlet transmissivities at different depths from 17 July to 16 August 2006……62
Figure 44. Discharge (Q) and suspended sediment concentrations (SSC) compared with mooring C transmissivities at different depths from 17 July to 16 August 2006……63
Figure 45. Surface sediment plume progression…….……...66
Figure 46. The elongation of surface sediment plumes……..…67
Figure 47. Minimal extent of sediment plumes (outlined) coinciding with northerly winds……..68
Figure 48. Cartoon of a proposed mechanism for obtaining overflow and underflow currents without intermediate interflow currents……...72
Figure 49. Gelifluction lobes on the western shore of Linnévatnet.……..……76

ABSTRACT

High Arctic sedimentary processes in a distal, proglacial lake (Linnévatnet, Spitsbergen, Svalbard) were studied in July and August of 2006 to understand links between climatic controls and suspended sediment entering the lake. Linnévatnet, one of the largest lakes in Svalbard (4.7 km long, 35 m deep), contains sediments dating from the late Pleistocene. Previous studies have attempted to quantify annual sedimentation rates and calibrate the lake's lamination, however much remains unknown about the suspended sediment entering the lake from the south, and the seasonal mechanisms and processes of sediment deposition into the basin. This study provides a better understanding of summer sedimentation patterns in Linnévatnet, which in turn enables enhanced interpretations of the long-term Svalbard climate record preserved in the Linnévatnet sediment cores. Depth, temperature and transmissivity (turbidity) were recorded in water column profiles by a Seacat SBE 19 profiler over a three-week period. A local automated meteorological station recorded air temperature, wind direction and velocity, precipitation, and solar radiation. Additionally, an automated camera recorded images of the lake inlet to document changes in the inflow stream and the occurrence of surface sediment plumes. Vertical water column profiles reveal that Linnévatnet is dominated by overflow density currents near the lake inlet, while underflow density currents were detected distal to the inlet. Delta turbidity flows were also detected. The sediment plumes fluctuated in great breadth and depth, though they could not be directly constrained to individual meteorological conditions. As a second objective, a baseline study of the Linnévatnet thermal regime was performed. Lake temperatures reached 6.5ºC, surpassing previously speculated temperatures for this High Arctic meltwater lake.

1. Introduction

1.1 Purpose

The purpose of this study is to identify the meteorological effects on sediment transport processes in Linnévatnet, a High Arctic, distal glacial-fed lake in Spitsbergen of the Svalbard Archipelago. These climatically sensitive sediment processes have never been studied in Svalbard, and High Arctic lake sedimentation is not well understood. Fieldwork for this study was conducted in conjunction with the 2006 Svalbard REU (Research Experience for the Undergraduate) Program, funded by the National Science Foundation. The objective of this REU program was to conduct comprehensive research of modern geologic processes in the Linné valley (Linnédalen) system, comprising the glacier (Linnébreen), sandur and rivers (Linnéelva), and distal meltwater lake (Linnévatnet), in order to calibrate and interpret the extensive climate record confined within the lake sediments. Sediments have been dated as far back as late Pleistocene. This study provides a better understanding of summer sedimentation patterns in Linnévatnet, which in turn enables enhanced interpretations of the long-term Svalbard climate record, and ultimately, the climate record of the High Arctic.

1.2 Justification: Global Climate Change

Global climate change is a critical issue currently gaining an increasing spotlight in scientific and political realms. The average global temperature since the industrial revolution has risen approximately 0.6ºC, and carbon dioxide concentrations in the earth's atmosphere have increased by 35% (MacBean et al., 2004). The Intergovernmental Panel on Climate Change (IPCC) reports with certainty that there

exists a natural greenhouse effect and that human activities, namely fossil fuel combustion, amplify the greenhouse effects (Watson et al., 2001). The recent global warming is strongly affecting terrestrial biological ecosystems including such changes as earlier timing of spring events, such as leaf-unfolding, bird migration and egg laying, as well as poleward and upward shifts in ranges in plant and animal species (Adger et al., 2007). The IPCC found that the anthropogenic uptake of carbon has also led to ocean acidification (Adger et al., 2007). Offshore, oceans are Insolation, atmospheric circulation, and volcanic aerosols have been insufficient to explain global climate changes, suggesting the influence of anthropogenic factors on the current temperature increase (e.g. Serreze, 1999; Watsen et al., 2001). Furthermore, the IPCC proposes that global temperatures will rise an additional 1.4ºC to 5.8ºC in this century if greenhouse gasses continue to be added to the atmosphere at their present rate (Watsen et al., 2001). Recent studies report increasing global temperatures, with 2005 recorded as the warmest year in the instrumental record beginning in 1880 (Francis et al., 2005; Richter-Menge et al., 2006)

The Arctic is a particularly important region to study climate change because of its sensitivity to slight changes in climate (e.g. McBean et al., 2004; Watsen et al., 2001). This sensitivity is the result of a dynamic series of mechanisms. First, ice and snow have a much greater albedo than water and soil. As temperatures rise and ice and snow cover decrease, the water and soil surface areas increase, thereby absorbing more radiation, causing greater warming; this is described as a positive feedback loop. Second, heat radiation absorbed by the ocean transfers back to the atmosphere at a greater rate as sea ice decreases and disappears (McBean, 2004). Positive feedback loops, which also

include cloud dynamics, tend to trap and enhance temperature anomalies (Overpeck et al., 1997). Lastly, the Arctic region significantly influences the climate of the rest of the globe due to atmospheric and oceanic circulation patterns (Perreault, 2006). The affects of climate change in the Arctic have the potential to cause significant global climatic shifts resulting in serious worldwide effects.

Climate change effects have been readily detected and recorded in the Arctic. The sea ice extent in September 2005 was the minimum observed summer extent, while the sea ice extent observed in March 2006 was the minimum observed winter extent throughout the satellite era (originating in 1979) (Richter-Menge, 2006. The rate of temperature increase in the Arctic is twice that of global increase, with winter temperatures in some areas of Alaska and Canada rising 3°C to 4°C in the past four years (McBean et al., 2004). Serreze et al. (1999) have gone as far as calling the Arctic a net carbon dioxide source instead of a sink. Furthermore, permafrost temperatures are continuing to increase, tundra vegetation greenness is on the rise, and the Arctic provides a large contribution toward the increases in temperature (Richter-Menge, 2006).

1.3 Site Description

Svalbard is an archipelago in the Arctic Ocean, located between latitude 74ºN to 81ºN and longitude 10ºE to 35ºE, halfway between the North Pole and Norway (Figure 1). The total land area of Svalbard is 62,160 km^2, and approximately 60% of the area is glaciated (Ingólfsson, 2004). Spitsbergen is the largest of the islands, with an area of 37,673 km^2 (Official Statistics of Norway, 2005). The Spitsbergen landscape is characterized by glacially eroded fjord systems and rugged mountains with steep

gradients. The warm West Spitsbergen Current, a branch of the North Atlantic Current, moderates a slightly warmer and more humid climate than other Arctic areas, yet permafrost thicknesses range from 10-40 m near the coast to over 450 m in the highlands (Ingólfsson, 2004). The mean annual air temperature at study site Kapp Linné, Spitsbergen, is -5ºC, averaging -12ºC in the winter and +5ºC in the summer (Perreault, 2006). The mean annual precipitation is about 40 cm, predominantly in the form of snow (Ingólfsson, 2004). It is important to note, however, that there are inherent difficulties with measuring snowfall, so these measurements are only an approximation (Snyder et al., 2000).

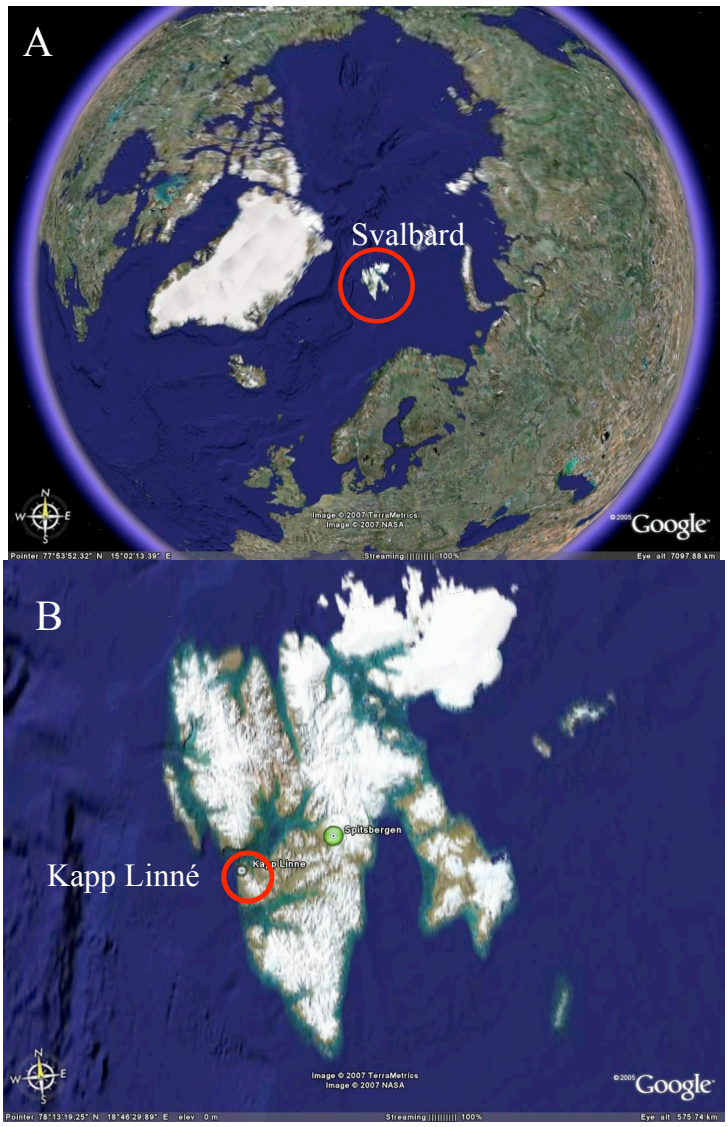

Figure 1. Global view of Svalbard (A) and study site Kapp Linné at Spitsbergen (B).

1.3.1 Linnédalen

Linnédalen is a tributary valley of Isfjorden located on the western shore of Spitsbergen (~73.3ºN, 13.5ºE)(Figure 2). It is 15 km long and 2 km wide, bound on both sides by ridges of approximately 500 m relief. This valley was once an arm of Isfjord until isostatic rebound, resulting from deglaciation, isolated Linnédalen (Landvik et al., 1987). Radiocarbon ages of marine mollusks suggest that the lake basin deglaciated

about 9,000-10,000 yr bp. (Mangerud and Svendsen, 1990). The valley glacier Linnébreen (1.7 km^2) sits at the southern end of the north-south trending valley. Previous work suggests that Linnébreen is melting at a rapid rate, and has an annual negative mass balance since at least the mid 20^{th} century (Helfrich, 2007; Schiff, 2005).

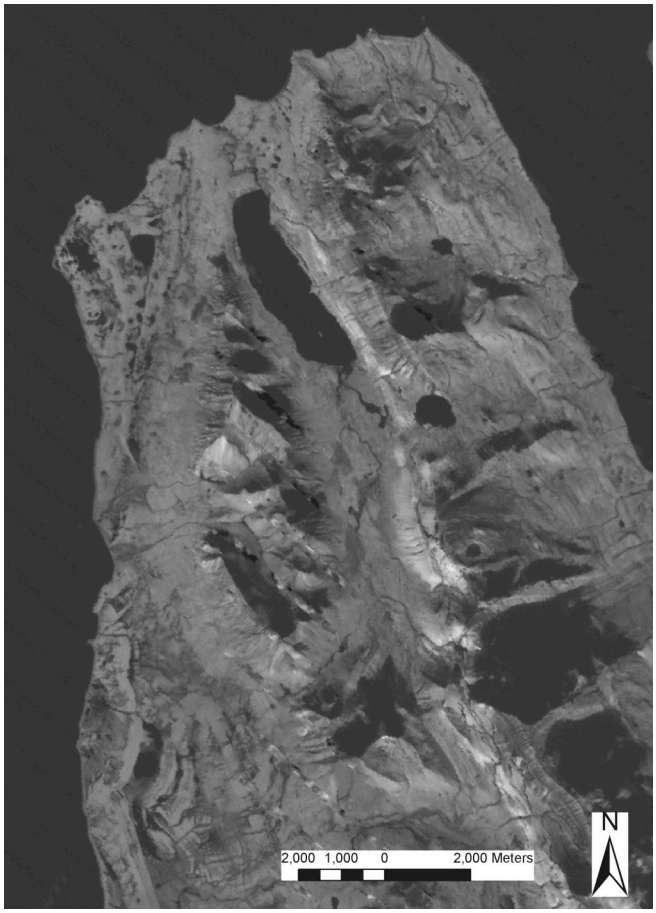

Figure 2. Satellite image of Linnédalen Valley. The Linnébreen glacier is ~ 8km upvalley from the lake. Image from Gercke (2006).

1.4 Tectonic Background of Linnédalen

Svalbard, often known as a 'mecca' for geologists, has a rich and long geologic history. There are continuous bedrock sections in Svalbard that span more than 11 km and more than 1 km high. These sections are located along the southern shore of Van Mijenfjorden. The following paragraph is a summary of the geologic history of Svalbard from Ingólfsson (2004) and Johnsen et al. (2007). The basement rocks of Svalbard, including Precambrian, Cambrian, and mid-Silurian strata, occur as a belt along Spitsbergen's west coast. This basement rock is traditionally called the Heckla Hoek series, characterized by arétes of metamorphic material. Tillite on Svalbard was deposited when Spitsbergen was situated near the South Pole approximately 600 Ma. The Caledonian Orogeny influenced subsequent large-scale folding and faulting as Svalbard was near the equator. About 400 Ma, during the Devonian, Svalbard was located just north of the equator; more than 8 km of sandstones, conglomerates, and shales were deposited in near-shore environments, deltas and lakes. Devonian beds often consist of red sandstone, representing an arid environment. In the Carboniferous, Svalbard continued moving north, away from the desert climate of the Devonian and into one more tropical. Vegetated swamps and flood basins were common during this time, as was the associated deposition of carbonates and red alluvial sandstones. During the Permian, a marine transgression occurred as Svalbard continued moving north. Shallow-water marine areas periodically became dry, resulting in marine carbonates containing shells and sponges, as well as evaporites. In the Mesozoic, the Arctic and North Atlantic Oceans began to open as what are now Europe and Greenland rifted apart. This rifting resulted in dolerite intrusions. The Svalbard climate throughout this time was temperate

and humid, with mostly marine deposits aside from the terrestrial igneous intrusions. During the Tertiary, Spitsbergen experienced local convergence as a result of tectonic transform faulting between Greenland and Svalbard. Lower Tertiary deposits consist of sandstones with abundant coal seams. At this time, the climate of Svalbard was getting successively cooler both as a result of the slow northward drift, and as a result of a late Tertiary global cooling. In the Quaternary, Svalbard was subject to repeated glaciations. Ingólfsson (2004) suggests that they may have been 50 or more glaciations since the onset of the cooler period, although the sediment record is poor due to the removal of older glacial deposits during subsequent glaciations.

1.4.1 Bedrock of Linnédalen

Within the Linnévatnet watershed, there are five distinct lithologies (Figure 3): Precambrian phyllite, Carboniferous coal-bearing quartzitic sandstone, late Carboniferous-Permian dolostones and limestones, Late Permian silicified shales and siltstones, and Mesozoic dolerites (Dallman et al., 1992). The topographic highs on the western side of the Linnédalen valley are dominated by Precambrian areno-argillaceous phyllite (commonly called Heckla Hoek) (Ohta et al., 1991). The central valley floor is composed of early Carboniferous quartzitic sandstones representing alluvial and fluvial deposition into fault-bounded basins (Dallman, et al., 1992). The eastern side of the valley is primarily dominated by interbedded dolomites, limestones, dolomitic sandstones and gray shales of the late Permian, representing a marine transgression sequence (Dallman et al, 1992); marine fossils are commonly seen. High up on the eastern ridge is an outcrop of late Permian silicified shales, siltstones and sandstones, representing a

transition from shallow marine to low-energy, oxygenated shelf deposition (Dallman et al., 1992). Lastly, a Mesozoic dolerite sill is exposed on the eastern side of the valley, approximately 100 m above Linnévatnet (Dallman et al., 1992).

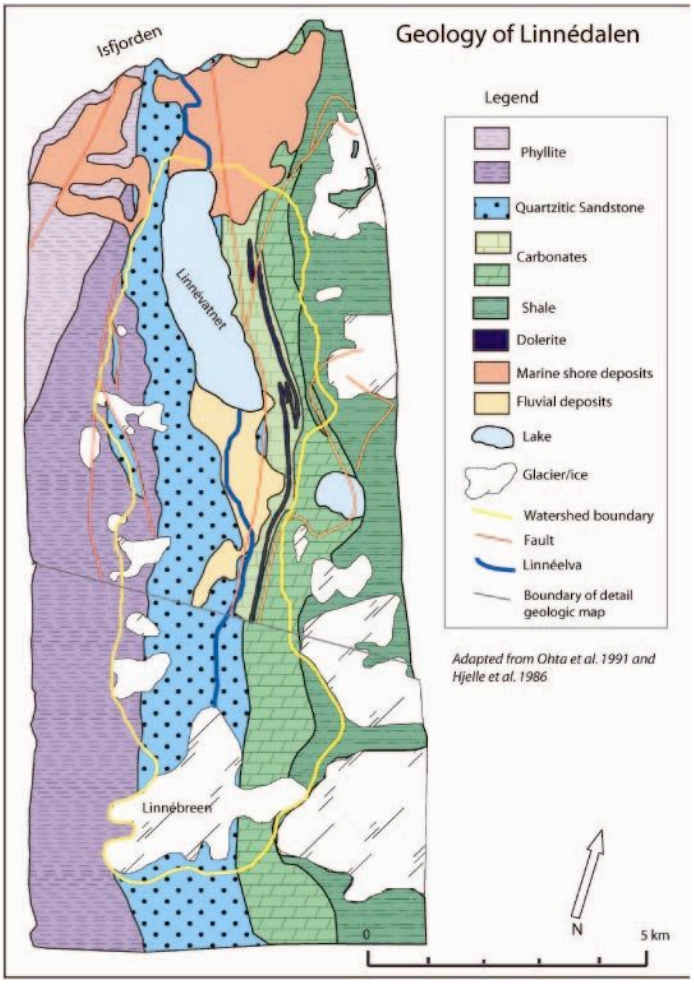

Figure 3. The geology of Linnédalen. From Perreault, 2006.

1.5 Components of Linnédalen

1.5.1 Glacier Linnébreen

The present day terminus of Linnébreen lies 1.2 km behind its Little Ice Age (LIA) terminal moraine complex. The moraine complex is composed of till (the grain size ranges from silt to large boulders). Using lichenometric dating, Werner (1993) found that there were four periods of glacier stabilization in the late Holocene: 1500 ya, 1000 kya, 650 ya, and again during the LIA. The lichens were assumed to start growing on the moraine material after the glacier had stabilized, and were dated by size using established growth curves (Werner, 1993). Other terminal moraines on Spitsbergen were found to be of the same ages using other dating techniques (Svendsen and Mangerud, 1997). Linnébreen retreat has occurred primarily during the past century; an aerial photo (Figure 4a) taken in 1936 shows Linnébreen against its moraine, while a 1995 photo shows the terminus far behind the moraine (Figure 4b). Work by Matell (2006) suggests that the glacier area has been reduced by 60% since the 1930s – twice the regional retreat rate. Schiff (2004) estimated the area and volume as 1.7 km^2 and 0.072 km^3, respectively.

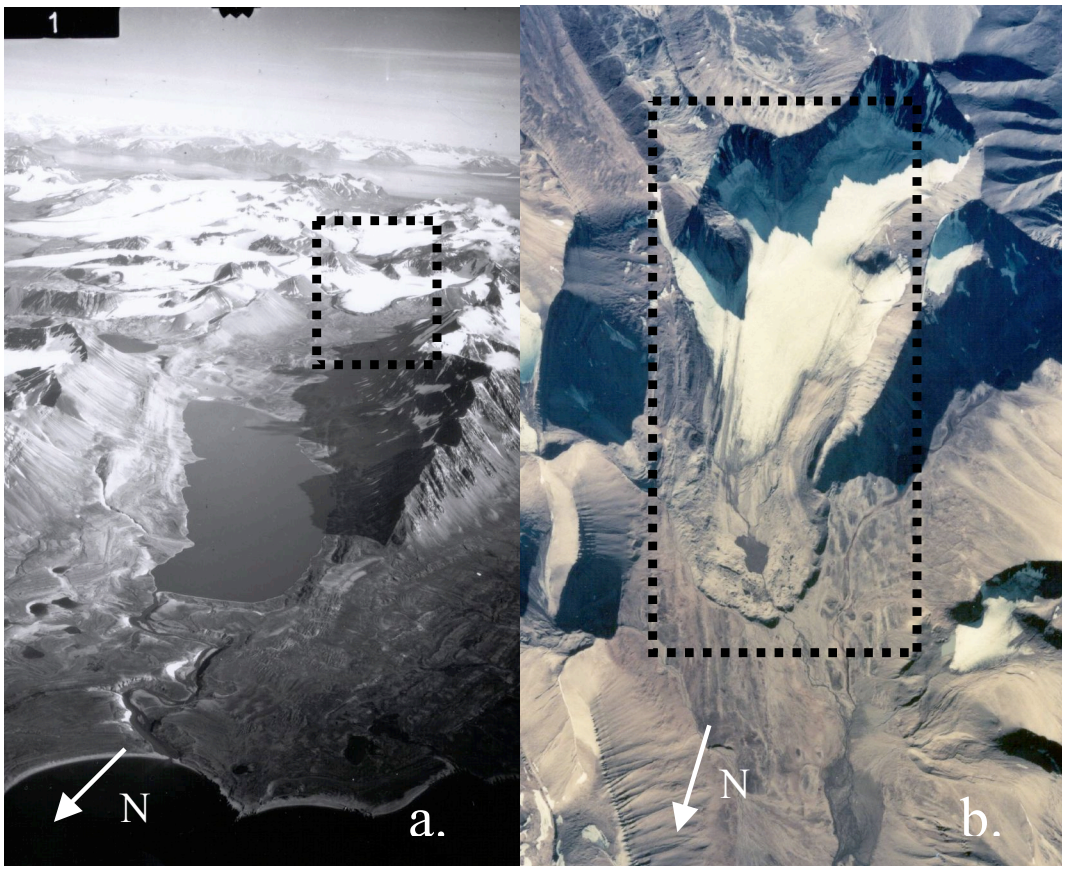

Figure 4. Oblique aerial photographs of the Linnébreen glacier in the Linné valley (a) in 1936, (b) in 1995. Notice the glacial retreat. Images from Norsk Polarinstitutt.

1.5.2 River Linnéelva

Linnéelva originates as two lateral streams off Linnébreen that meet in front of the terminus. This area has an abundance of fine sands, silts, and clays, as well as clasts of sandstone and phyllite up to 50 cm in diameter (Matell, 2006). The sands are fine because they are products of weathered fine-grained sandstones. The silts are a result of glacial activity over the bedrock, and the clays are from a combination of physical and chemical weathering of abundant phyllites of the west ridges. After passing through the an incision of the LIA terminal moraine, Linnéelva breaks into a complex braidplain. In the summer months, the mean braidplain width is approximately 300 m, with single braid strands averaging 1 to 15 m across, rarely deeper than 50 cm. Cobbles and pebbles are

the dominant grain sizes, although sand and silt deposits are visible in areas of eddies and isolated pools during low flow. The braidplain extends about 2.5 km downstream, until it hits a bedrock ridge and spreads out into a low gradient area. The water velocity decreases and pools as it increases in breadth, approximately 1.5 km downstream from the braidplain. In this area, the deposition of suspended silts is recorded (Mattel, 2006). As Linnéelva passes over the bedrock ridge, the gradient increases, thereby decreasing the stream width, channelizing the flow, and increasing the velocity. Now approximately 6 km downstream from the Linnébreen, the gradient decreases, widening the stream to approximately 70 m; depths range from 10 to 50 cm. A wave-dominated delta composed mainly of clasts of phyllites, carbonates and sandstones, lies at the southern end of Linnévatnet.

1.5.3 Lake Linnévatnet

At the northern end of Linnédalen is the lake Linnévatnet. Linnévatnet is elongate roughly north-south, approximately 4.7 km long, and 1.3 km wide, with an elevation of 12m above sea level (Bøyum et al., 1978). The lake developed in a glacially over-deepened basin more than 9,000 yr bp when the glacier extended to the ocean (Svendsen et al., 1989). Several projects used acoustic profiling to create a bathymetric map (figure 5) and an isopach map (figure 6) (Bøyum et al., 1978; Werner, 1988; Svendsen et al., 1989; Roof, 2003). The lake bottom is characterized by three distinct basins. Two of the basins, located at the southern end of the lake, are relatively shallow and divided by a bedrock high which extends into an elongate island (Snyder et al., 2000). The deeper third basin, located in the northern end of the lake, is twice the depth

of the shallow basins at approximately 37 m. The major water and sediment inflow for the lake comes from the braided streams of Linnéelva. Additionally, a smaller nival melt stream from a western valley cirque enters the lake in the southwestern corner. A few ephemeral streams also enter the lake from the eastern and western valleys. The lake outlet is at the northeastern corner of the lake and drains into Isfjorden, nearly 2 km north of Linnévatnet.

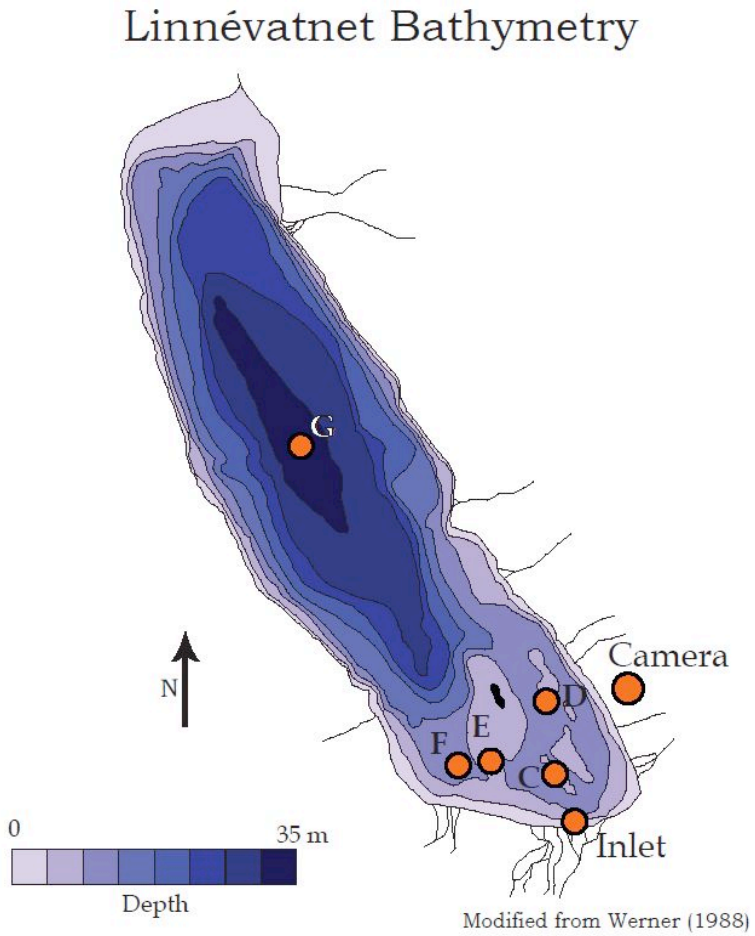

Figure 5. Bathymetry of Linnévatnet with superimposed position of each mooring location and camera placement.

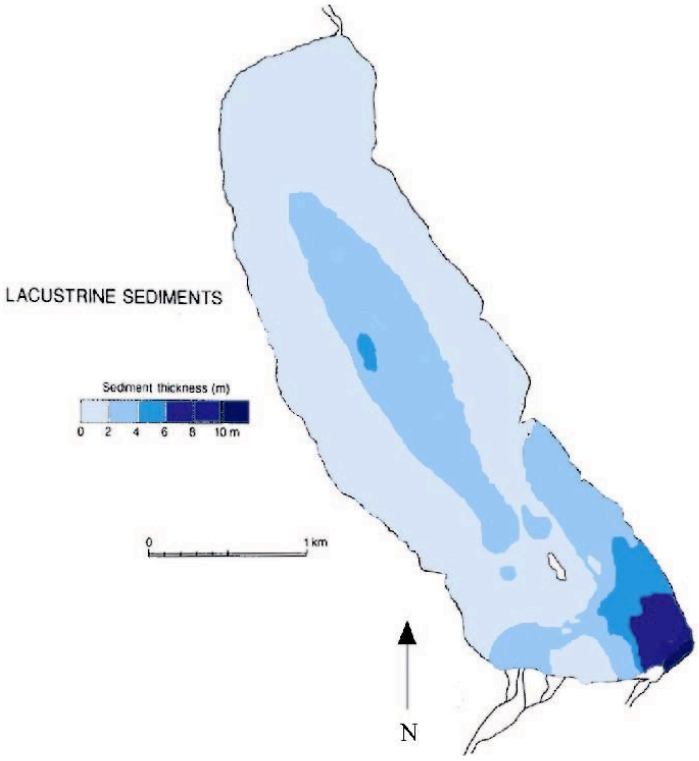

Figure 6. Isopach map of sediments in Linnévatnet. Simplified from Svendsen et al., (1989).

1.6 Sediments in Linnévatnet

Laminated lake sediments in proglacial environments serve as important proxies for changing climates. Most deposition occurs in the spring and summer months, as coarse grains become mobilized by higher-energy meltwater streams and rivers, while in the winter months, the fine sediments are deposited as a result of settling; this coincides with Hjulström's diagram (in Boggs, 2001). The seasonality difference in deposition creates distinct annual couplets (Matell, 2006). Diurnal and annual changes in meteorological conditions including temperature, radiation, and precipitation, affect glacial melt and the amount of sediment transported to proglacial lakes. Thus, by

examining changes in thicknesses, grain sizes and mineralogies, laminated lake sediments are used to interpret changes in climate.

Because of its rich paleoclimate record, researchers have extensively characterized the sediments contained within Linnévatnet. The sediment in Linnévatnet represents about 9,000 years of lacustrine deposition (Svendsen et al., 1989). Below the lacustrine sediment lie marine sediments (Svendsen and Mangerud, 1997). The maximum lacustrine sediment thickness within Linnévatnet is approximately 12 m, occurring at the proximal south delta (Svendsen et al., 1989); sediment thickness decreases with progressive distance north of the delta. The upper 80 percent of the lacustrine sediments are laminated (Werner, 1988; Svensen et al., 1997; Snyder et al., 2000).

The actual transportation and deposition of suspended sediments in Linnévatnet is poorly understood. By studying modern processes which control the supply, transport, and deposition of sediment, relationships may be formed between processes and suspended sediment concentrations. Ultimately, studying modern processes leads to more accurate interpretations of Linnévatnet's lamination stratigraphy.

1.7 Discharge and Suspended Sediment

Hysteresis occurs when there is a change in the relationship between discharge and suspended sediment concentrations (SSC). Clockwise hysteresis (Figure 7) describes decreasing SSC in time – flows of the same magnitude carry less sediment. Sediment depletion over time is suggested in clockwise hysteresis. Seasonal clockwise hysteresis is generally caused by the depletion of available sediment in a watershed (Maizels, 2002).

The influence of diurnal cycles from solar radiation, variations in the contribution of tributary streams, and short-term sediment storage are also main factors of hysteresis. Lewkowicz and Wolfe (1994) revealed that as discharge falls after a daily diurnal peak, sediment is deposited in channels and then becomes entrained the next day.

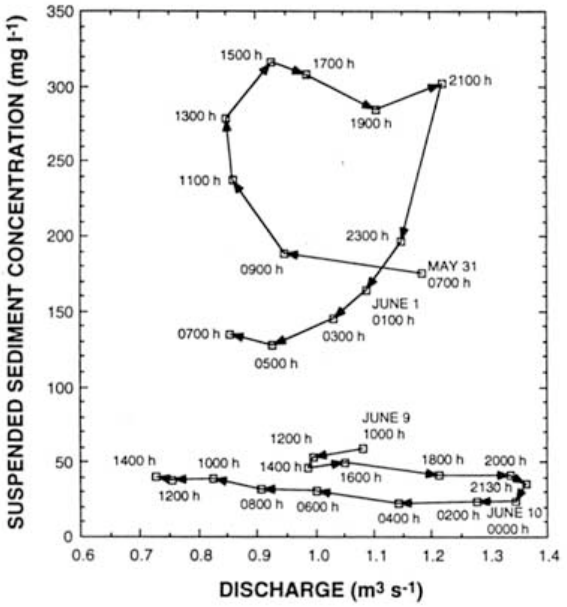

Figure 7. Suspended sediment hysteresis. Two episodes of clockwise sediment hysteresis observed on Ellesmere Island, early summer 1991. Greater discharge is required to obtain the same SSC over time. From Lewkowicz and Wolfe (1994).

Suspended sediment transport is additionally influenced by peak flow events. Summer Svalbard REU undergraduate students, Carr (2007) and Roop (2007), are researching the cause of peak flow events in Linnévatnet. Generally, during high flows, the stream competence increases, allowing the transport of much greater quantities of sediment; a day of high flow can transport more sediment than a week of low flow. Hardy (1996) found that in a watershed on Ellesmere Island, over half of the annual load was delivered in 3 to 4 days, and 99 percent of the load was delivered in 15 to 20 days.

In basins that do not experience sediment exhaustion, sediment load is typically transport-limited. In this case, short term storage and release of sediment is particularly important. The sources and sinks are typically inconstant during a single season. Hodson and others (1998) found that the Spitsbergen glacier Auestre Brøggerbreen was a source as well as a sink of fine sediment; the sandur changed from a minor sediment source in the early summer to a major sediment sink of deposition in the mid- to late summer.

1.8 Hydroclimate: Stratification & Currents

1.8.1 Lacustrine Stratification

Sedimentation processes in high arctic proglacial environments have been studied very little. As such, high arctic lacustrine processes are inferred from arctic lakes with nival regimes, as well as temperate proglacial lakes (Lewis, 2000). Most arctic lakes are described as cold-monomictic – lake temperatures never exceed 4ºC, and may only experience one overturn circulation period per year (Wetzel, 1983). At 4ºC, freshwater contains its greatest density. Thus, freshwater lakes overturn in the fall as the surface water cools to 4ºC. Cold-monomictic lakes warm in the summer months resulting in ice

break up, but no consequent density stratification. Dimictic lakes, mainly temperate water bodies, experience complete mixing on a twice-annual basis (Cohen, 2003). Lakes referred to as meromictic mix only incompletely. Meromixis affects sedimentation by creating a chemocline, a density barrier, on top of which sediment may travel horizontally before deposition. Rettelle and Child (1996) found that chemoclines can create an even accumulation of clastic sediments across a lake bottom.

1.8.2 Currents

A river entering a lake may have a different density than that of the lake, causing density currents. These currents may float on the surface of the lake as an overflow current, descend to an intermediate depth as an interflow current, or descend to the bottom of the lake as an underflow (Figure 8). Differences in densities between the river inflow and the lake water may result from temperature, salinity, or suspended load variations. According to Smith and Ashley (1985), overflows may be more frequent in basins receiving very fine sediments or those with low detrital input.

By spreading throughout the lake at intermediate depths, interflows are effective at distributing sediment, and interflow deposits thin from proximal to distal locations (Lewis, 2000). The coarser sediments tend to be deposited rapidly near the lake inlet, while the silts and clays are carried farther (Smith and Ashleigh, 1985).

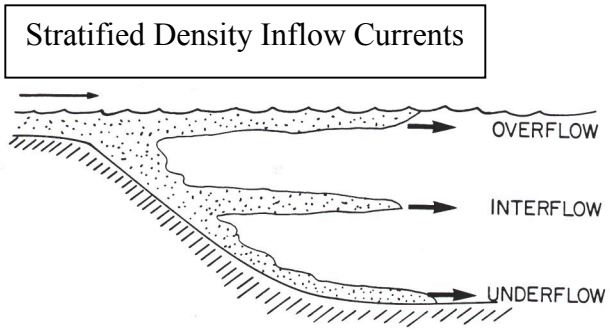

Figure 8. Sketch of inflow mixing patterns in glacier-fed lakes. Modified from Smith and Ashley (1985).

Similarly, underflows occur when sediment loads entering the lake are great (Cohen, 2003). In many proglacial lakes, underflows are the dominant processes for sediment transport and deposition (Smith and Ashley, 1985). Temporal variation in interflow and underflow suspended sediment may create intra-annual rhythmites on the lake floor, leading to potentially complex and difficult paleoclimate interpretations. Varve detection may be thrown off by intra-annual rhythmites and turbidites, but these [chaotic] deposits may undoubtedly have paleoenvironmental significance with regard to snowmelt, glacial discharge, and precipitation.

In addition to overflows, interflows, and overflows, which are grouped together as stratified inflow currents, there are also homopycnal inflow currents (figure 9). Homopycnal currents occur as a uniform density and turbidity through the entire water column. According to Smith and Ashley (1985), homopycnal flows are uncommon in non-ice-contact lakes and are "probably confined to mainly shallow, freely circulating lakes whose inflow density varies little, a feature not typical of glacier rivers."

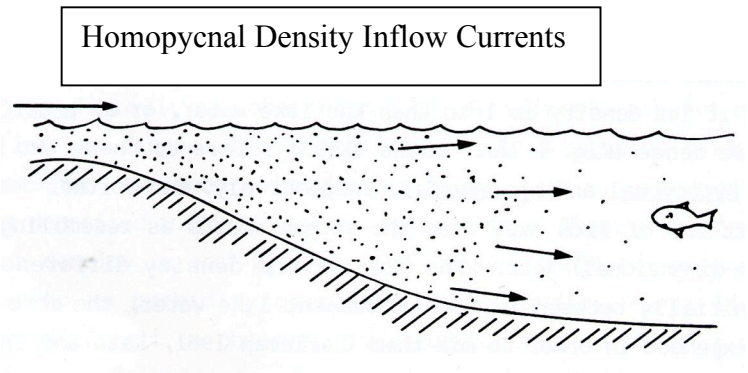

Figure 9. Sketch of homopycnal inflow mixing in meltwater lakes. Modified from Smith and Ashley (1985).

A distinction must be emphasized between turbidity currents generated directly from inflow, and those created by slope failure. Gravity flows are important mechanisms for the transport of sediment in many lakes. They frequently form in association with influent rivers. Turbidity flows, the most frequent gravity flows in lakes, form when sediment-rich underflows travel down a sloping delta surface, or by the partial resuspension of unsteady soft sediment on a slope (Cohen, 2003). Additionally, rapid changes in underflow inertia, or local steepening, can trigger secondary gravity flows in deltaic sediments (Pickrill and Erwin, 1983). Turbidity flows can travel over large areas due to little frictional resistance to flow. Sublacustrine fans result from the settling of extensive lobate delta deposits. Giovanoli (1990) and Scholz et al. (1993) found that turbidity flows are frequently erosive in lakes and may produce extensive sub-lacustrine channels, especially along high-gradient lake bottoms.

The Linnévatnet water body may be greatly influenced by wave action from wind. Waves are periodic oscillations and occur both at and below the lake's surface, and are active on many spatial and temporal scales (Imboden and Weüst, 1995). Understanding the influence of waves on Linnévatnet is important from a paleolimnological perspective

because the shallow-water waves can entrain and transport sediments, which influences the lake sedimentary record (Cohen, 2003).

Additionally, the Coriolis (or geostrophic) effect has an influence on the lake sedimentation; the Coriolis effect increases toward the poles. As a result, suspended sediment in the northern hemisphere moves counter clockwise about the lake.

Lake processes are extremely complex and must be thoroughly studied to understand how sediment is transported and deposited. The unique character of a lake is expressed through external controls such as watershed geology, vegetation, glacial cover, temperature, precipitation, and wind, and internal controls such as temperature, ice cover, and salinity (Lewis, 2000). In the High Arctic, even less is known about the complex transportation and deposition processes.

2. Methods

2.1 Fieldwork

The field season in Linnédalen took place between July 18th and August 14th, 2006. Meteorological and hydroclimate measurements are recorded by: 1) an automated meteorological station and supplemental temperature sensors, 2) vertical water column profiles, 3) water temperature data loggers, 4) water level data loggers, and 5) an automated remote camera.

2.2 Meteorological Station

Meteorological data is collected from a main automated Hobo® weather station 500 m south of Linnévatnet (T_1)(Figure 10). The station was erected in November, 2005 by the previous year's REU team, and it has been continuously recording since then. This study focuses only on data recorded during the 2006 field season. The weather station records air temperature, wind velocity and direction, barometric pressure, liquid precipitation, soil temperature, and solar radiation. The air temperature and barometric pressure sensors are approximately 2 m above ground. The temperature sensor is shielded from direct sunlight. Soil temperature sensors are 0.5 m and 1.5 m below the surface. Wind speed and direction, precipitation, and solar radiation sensors are 3.5 m above ground. The Hobo® station was assembled in accordance with specifications from the manufacturer, Onset Corp. All sensors are synchronized and record at 30-minute intervals. The Hobo® station normally measures relative humidity, however the sensor was damaged and recorded defective data. Thus, relative humidity measurements are not used in this study.

Additional Hobo® temperature and solar radiation loggers were emplaced up-valley. A temperature logger was located at the Little Ice Age moraine complex, 5 km south of Linnévatnet (T_m), and a temperature and radiation logger was located on the ice of Linnébreen, 8 km south of Linnévatnet (T_g). The weather conditions on Linnébreen many times deviate from conditions downvalley at the lake. Accuracies, locations, and dates used for each logger are summarized in Table 1.

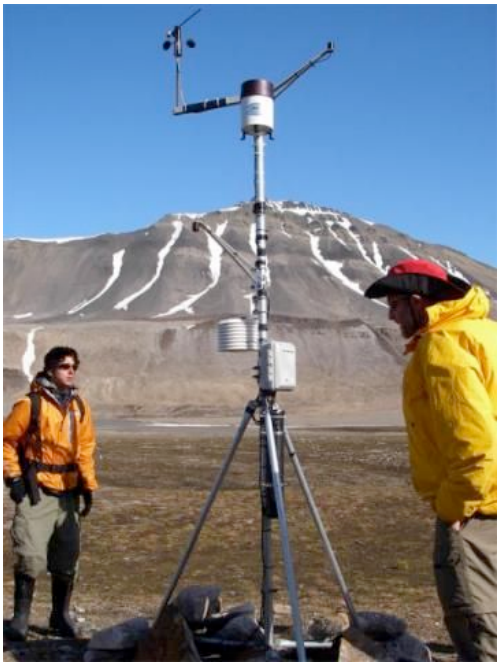

Figure 10. Automated weather station 500 m south of Lake Linné records meteorological conditions at 30-minute resolution.

Table 1. Weather Station Loggers, Linnédalen valley.

Logger	Location	Approximate Accuracy	Dates Used (2006)
Hobo® wx station temperature	T_l	±0.2º at 0º C	July 18 – Aug. 14
Hobo® wx station wind velocity	T_l	±0.5 m/s	July 18 – Aug. 14
Hobo® wx station wind direction	T_l	±5º	July 18 – Aug. 14
Hobo® wx station barometric pressure	T_l	±1.5 mbar at 0º C	July 18 – Aug. 14
Hobo® wx station liquid precipitation	T_l	±1% at up to 20mm/hr	July 18 – Aug. 14
Hobo® wx station soil temperature	T_l	±0.7º at 0º C	July 18 – Aug. 14
Hobo® wx station photosynthetic radiation	T_l	±5 umol/m^2/sec	July 18 – Aug. 14
Hobo® pro series temperature	T_m	±0.2º at 0º C	July 18 – Aug. 14
Hobo® pendant temperature and photosynthetic radiation	T_g	±0.5º at 0º C, ±5 umol/m^2/sec	July 25 – Aug. 14

2.3 Temperate Data-loggers

In July 2005, five moorings were deployed in Linnévatnet: moorings C, D, E, F, and G (Figure 6). Sediment traps and Hobo® water temperature data loggers were attached to the mooring ropes. The sediment traps were not used in this study. Temperature data loggers were fastened to the moorings at graduated depths. The moorings were secured to the lake bottom by ~ 80 lbs. rocks as anchors. They were pulled taught by buoys between 2 m and 3 m below the lake surface; the lake surface freezes in the winter. Mooring C, the closest mooring to the lake delta, was located approximately 0.25 km north of the lake inlet in a 15-m-deep basin. Water temperature loggers on C were positioned at depths of 2.5 m, 5.5 m, 9.5 m, 13.5 m, and on the underside of the anchor, 15 m. Mooring D was placed in a basin halfway between the lake island and the east shore, approximately 0.75 km northeast of the lake inlet.

Temperature loggers on this mooring were positioned at depths of 2 m, 5 m, 9 m, 13 m, and on the underside of the anchor, 15 m. Mooring E was deployed approximately 0.5 km northwest of the lake inlet, on the shallow basin divide. Temperature loggers on mooring E were located at depths of 3 m, 4 m, and on the bottom of the anchor at 5 m. Mooring F was positioned north ofthe basin divide, 0.75 km northwest of the lake inlet. Temperature loggers were fastened at 3 m, 6 m, 9 m, and on the bottom of the anchor, 10 m. The fifth mooring, G, was the most distal from the delta. It was deployed into the central basin approximately 3 km from the lake inlet. Temperature loggers on this mooring were positioned at depths of 3 m, 10 m, 20 m, 30 m, and on the bottom of the anchor at 35 m depth.

The Hobo® water temperature data loggers synchronously recorded lake temperatures at 30-minute intervals, with an accuracy of ±0.2ºC.

2.4 Water Column Profiles

Measurements of depth, temperature, conductivity, dissolved oxygen, and light transmission in the Linnévatnet water column were acquired by a Seabird Instruments® Seacat® SBE 19 Profiler fitted with a 25-cm path length Sea-Tech transmissometer (Figure 11). The accuracy of the transmissometer is ±0.5% light transmission. The temperature sensor has an accuracy of 0.01ºC between -0.5ºC and +35.0ºC. The accuracy of the conductivity sensor is 0.001 S/m. For this study, we focus on water column depth and transmissivity. The Seacat® records two values per second. Vertical water column casts were achieved by lowering the instrument two meters per second into the water from a zodiac boat (Figure 12). Once the instrument met the lake floor, it stopped

recording and was pulled back up to the boat. Water profiles were sampled daily between 11:00 and 18:00, with some additional casts later in the day. Due to the number of simultaneous student projects and a limitation of rifles, identical water column sampling times were unobtainable during the field season.

Figure 11. Water column profiles of depth and % light transmission were measured with the Seabird Instruments® Seacat® SBE 19 Profiler. Boots in upper left corner for scale.

Figure 12. Vertical casts involved lowering the Seacat® into the water column at mooring sites throughout the lake.

Light transmissivity is used to indicate the relative suspended sediment concentration within the water column (e.g. Retelle et al., 1996). The vertical casts were deployed at all five Linnévatnet mooring sites, as well as intermediate sites throughout the lake. The intermediate sites were composed of "red boat," "halfway between inlet and red boat," "halfway between mooring C and red boat," "halfway between lake inlet and red boat," "halfway between red boat and eastern shore," and "western inlet" (Figure 12).

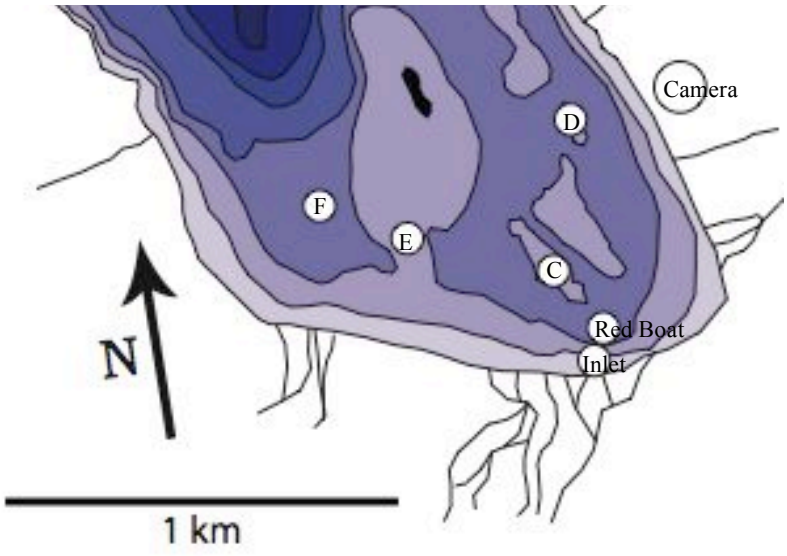

Figure 13. Mooring sites at the southern end of Linnévatnet.

The Seacat® data were downloaded and processed using the Seabird ® software. For analytical and graphing purposes, the data were averaged and sorted in 1-meter vertical groups.

2.5 Automated Imaging

An automated camera recorded images of the lake inlet to document changes in the inflow steams and the occurrence of near-surface sediment plumes. A Nikon® Coolpix 5700 was programmed to capture one image every three hours, for an 18-day period beginning 27 July 2006. The camera was positioned inside a padded, waterproof case with a glass window pane. It was powered by photovoltaic panels and an internal 35-aH gel cell sealed lead acid battery (Figure 14). This automated camera station was situated on a diabase sill outcrop northeast of the lake inlet, 100 m above the lake.

Figure 14. Programming the solar-powered automated camera to capture an image of the lake inlet every three hours.

2.6 Simultaneous Adjacent Projects

Other student projects surrounding Linnévatnet during the summer of 2006 included taking gravity cores of the lake sediment, deploying sediment traps at various depths on the lake moorings, and measuring discharge and suspended concentrations of Linnéelva river. Two other students worked on the mass balance and hydrology of the Linnébreen glacier.

3. Results

3.1 Weather Station

3.1.1 Air Temperature

Between 6 August 2005 and 14 August 2006, the air temperature in Linnédalen ranged from -22.60ºC to 11.77ºC, with an average of -1.5ºC. During the study season, between 18 July and 14 August 2006, the air temperature ranged from 3.74ºC to 11.77ºC. There were no month-long trends in air temperature from the beginning to the end of the field work period (Figure 15).

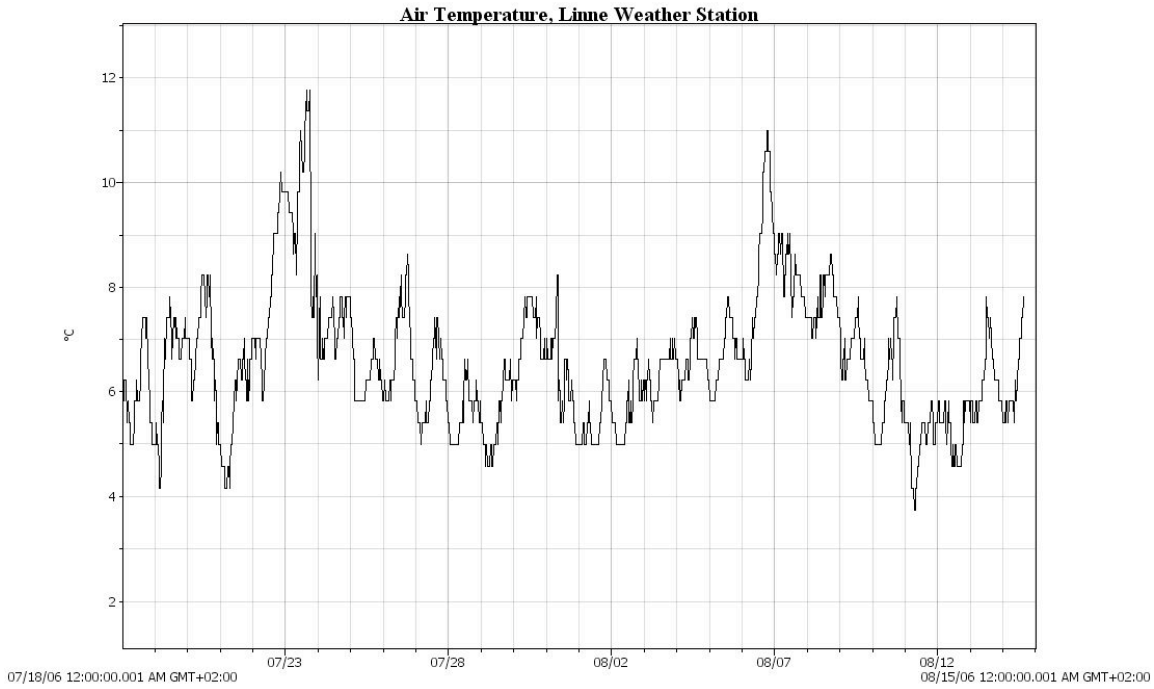

Figure 15. Air temperature in Linnédalen between 18 July 2006 and 15 August 2006.

3.1.2 Wind Velocity and Wind Direction

The fins and propeller detached from the wind sensors in the early winter of 2005, thus providing inadequate annual wind data. The equipment was repaired on the second

day of the study, 19 July 2006. The maximum wind velocity during the study was 8.91 m/s, the minimum was 0 m/s, and the mean was 2.11 m/s. The wind coming into north-south trending Linnédalen valley predominantly entered from N14ºE. However, the wind direction and velocities changed irregularly throughout the study. A noticeable change in air temperature accompanied the changes in wind direction. The southwesterly Atlantic Gulf Stream was considerably warmer than the polar winds from the north.

3.1.3 Precipitation

Approximately 425.2 mm of rainfall was recorded in Linnédalen valley between 6 August 2005 and 14 August 2006. Approximately 13.6 mm of rain were recorded during the field season (Figure 16). Of the 30 precipitation events recorded within Linnédalen, 29 occurred in August 2006. All precipitation events recorded comprised of 0.2 mm or more of rain. The highest accumulated precipitation in a 30-minute period was 0.8 mm.

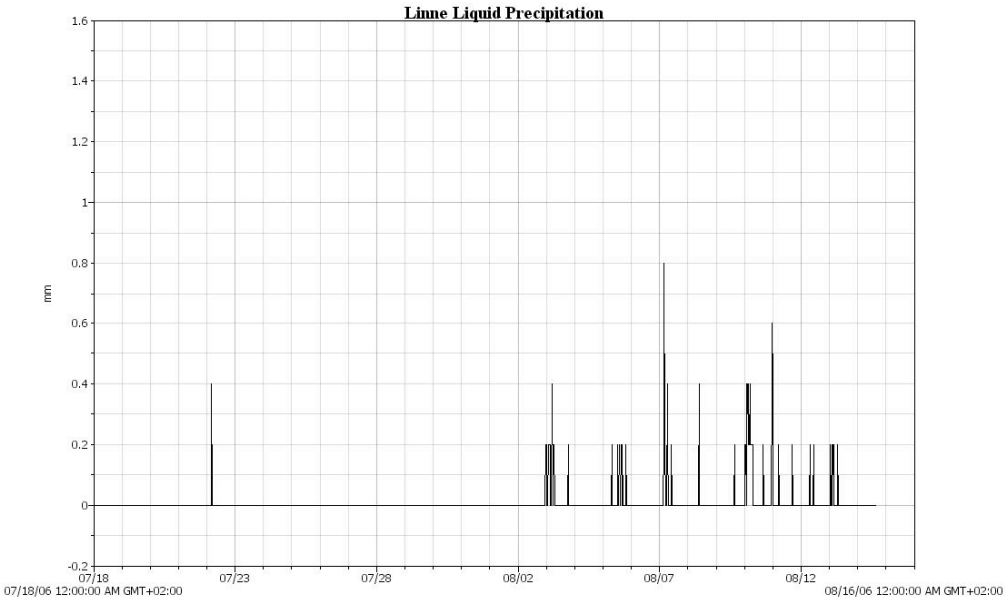

Figure 16. Rainfall in Linnédalen between 18 July and 15 August 2006. Total cumulative precipitation was 13.6 mm

3.1.4 Solar Radiation

The solar radiation in Linnédalen in July and August 2006, ranged from 1.9 W/m^2 to 604 W/m^2, with a mean of 116 W/m^2. Solar radiation was a function of cloud cover. There were diurnal radiation peaks due to the local valley topography and the path of the sun (Figure 17).

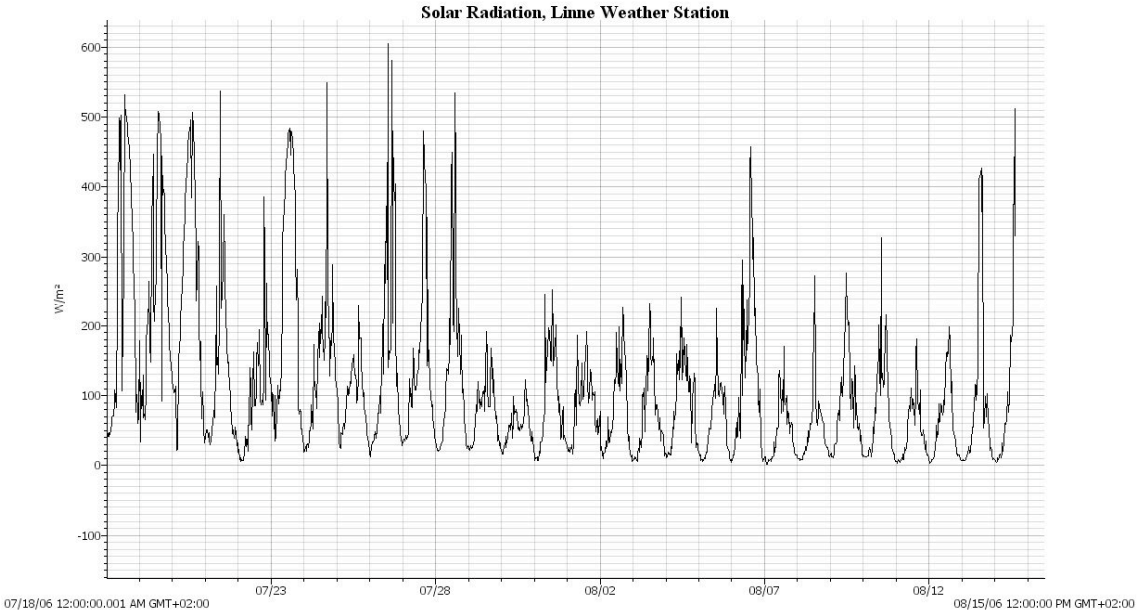

Figure 17. Solar radiation in Linnédalen between 18 July and 15 August 2006. Solar radiation may be a proxy for cloud cover.

3.1.5 Soil Temperatures

Discontinuous permafrost underlies the Linné valley floor. Soil sensors at 0.5 m and 1.5 m below the surface, in the active layer, reveal temperatures ranging from 4.6ºC to 6.7ºC, and 3.8ºC to 5.8ºC, respectively. Soil temperatures were predominantly influenced by surface air temperatures (Figure 18). The soil reached its coldest temperatures on 1 April 2006 with -10.33ºC 0.5 m below the surface and -8.86ºC 1.5 m below the surface. Figure 19 shows the point at which the soil 0.5 m below the surface changed from being cooler than the 1.5 m soil, to warmer than the underlying soil.

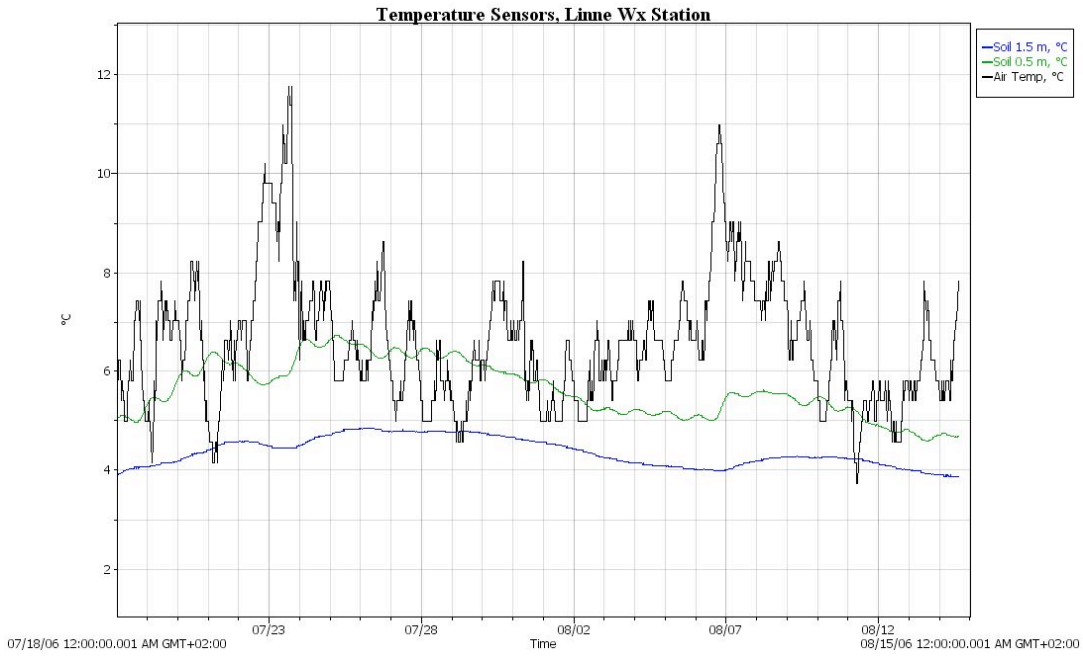

Figure 18. Soil temperatures from 18 July to 15 August 2006 at 0.5 m and 1.5 m below the surface. Note the influence of air temperature.

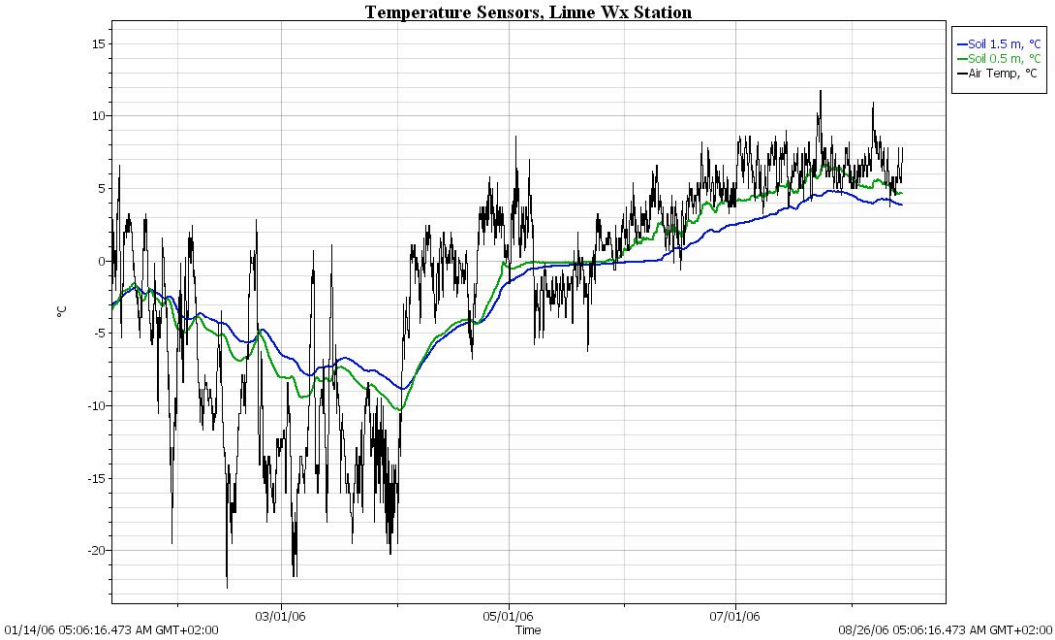

Figure 19. Soil temperature at 0.5 m and 1.5 m from 14 January 06 to 15 August 06. Note the lowest surface temperature if the year on 1 April.

3.2 Lake Temperature

Loggers on the five Linnévatnet moorings recorded water column temperatures since August of 2005. They revealed distinct seasonal characteristics (Figure 20). In September, the lake began a cooling period until mid October when the lake began to crystallize. The top two meters of the lake were frozen from late October until late April. In late April, ice began melting and was completely gone from the lake about 12 June. A warming trend continued throughout the summer of 2006. Linnévatnet was thermally stratified in the winter, however there was much mixing during the cooling and warming trends in the fall and spring, respectively.

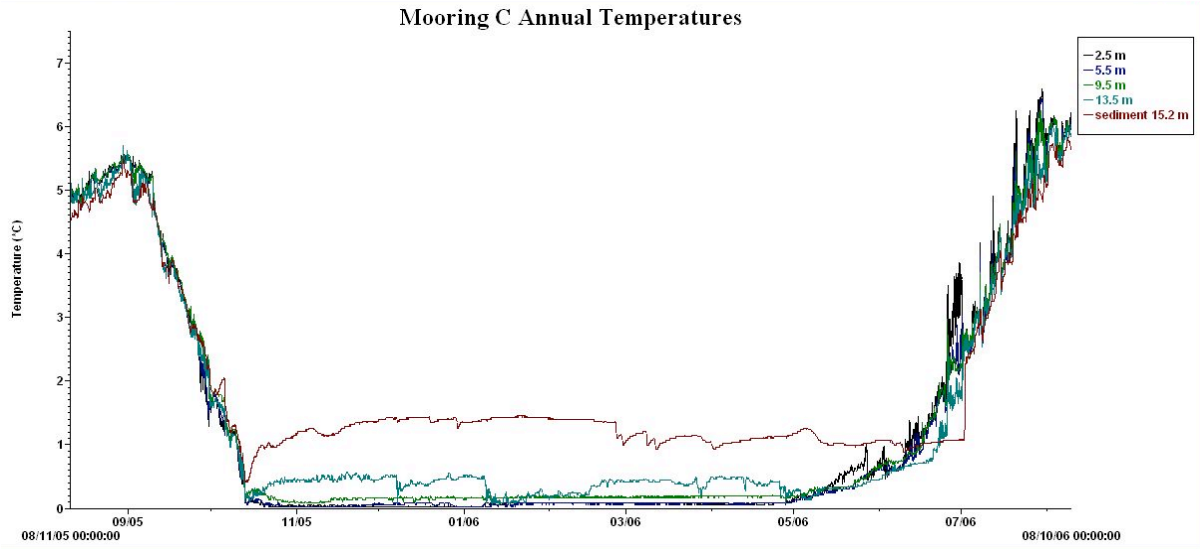

Figure 20. Linnévatnet temperatures from 11 August 2005 to 10 August 2006. The lake was frozen from mid-October to mid-June.

For the purposes of this study, we will focus on the lake temperatures in the summer field season. Water temperatures recorded at mooring C fluctuate from 3.8ºC to 6.5 ºC, with a broad trend of increasing temperatures (Figure 21). Additionally, a pattern of water cooling occurred approximately every four days. During this four-day cooling trend, water within the top 2.5 m varied by as much as 2.7ºC. At mooring D, these cooling patters were detected, but at a smaller scale, 1ºC (Figure 22). Two of the five temperature loggers on mooring D did not survive a year of deployment. These were located at 5 m and 15 m below the surface. Moorings E and F also indicate the period cooling within the broad warming trend (Figures 23 and 24). Depths of Linnévatnet at Moorings C, D, E, and F do not exceede15.2 meters. Mooring G, the deepest mooring (35 m), showed the least thermal stratification of all the moorings (Figure 25). The 3-m temperature logger was not recovered from mooring G.

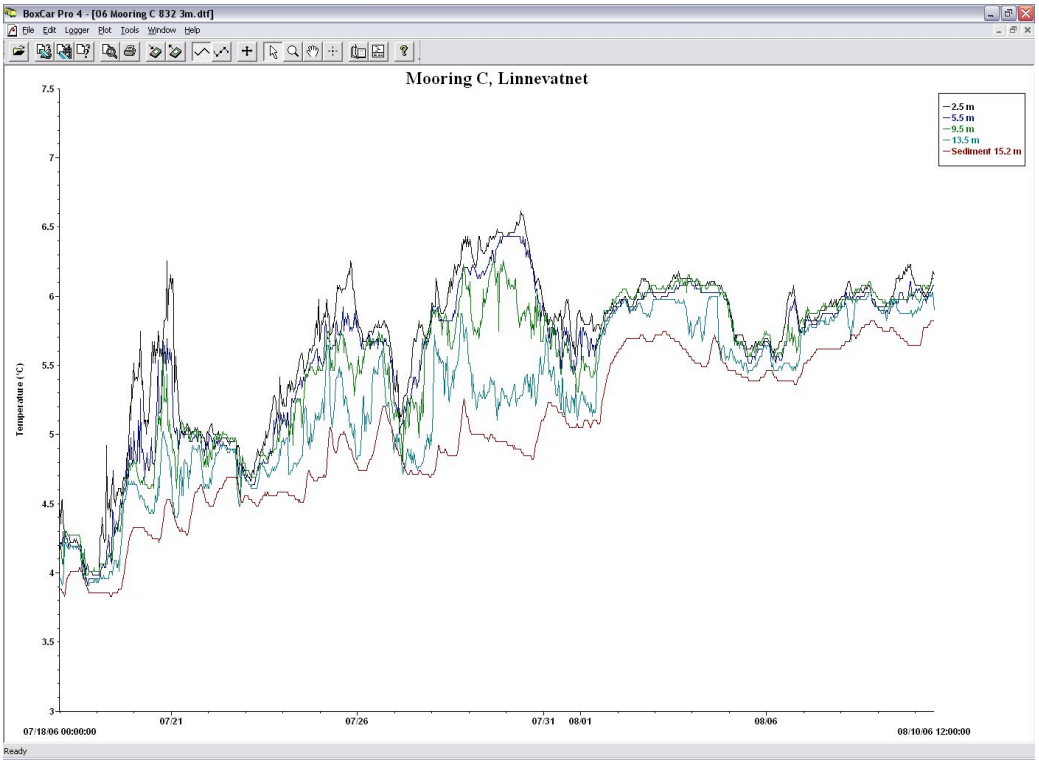

Figure 21. Water temperatures at mooring C from 18 July to 10 August 2006, at depths of 2.5 m, 5.5 m, 9.5 m, 13.5 m, and the bottom sediment at 15.2 m. Notice the thermal stratification for most of July and August.

Figure 22. Water temperatures at mooring D from 18 July to 10 August 2006, at depths of 2 m, 9 m, and 13 m. Notice the thermal stratification.

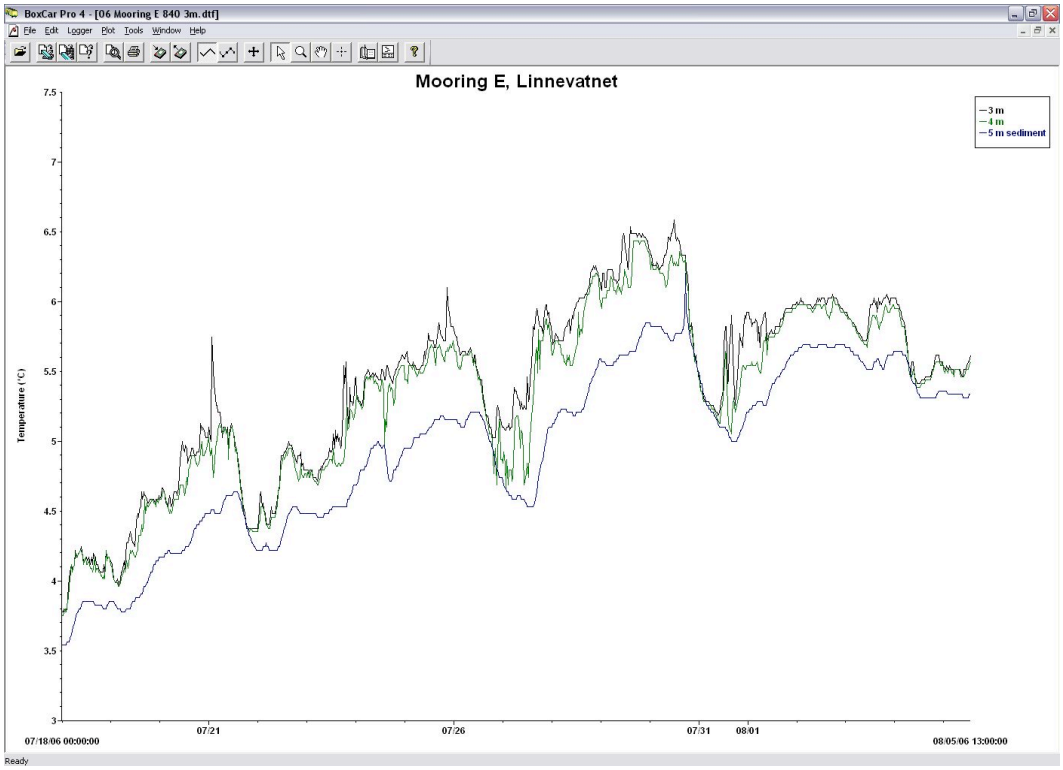

Figure 23. Water temperatures at mooring E from 18 July to 10 August 2006, at depths of 3 m, 4 m, and 5 m.

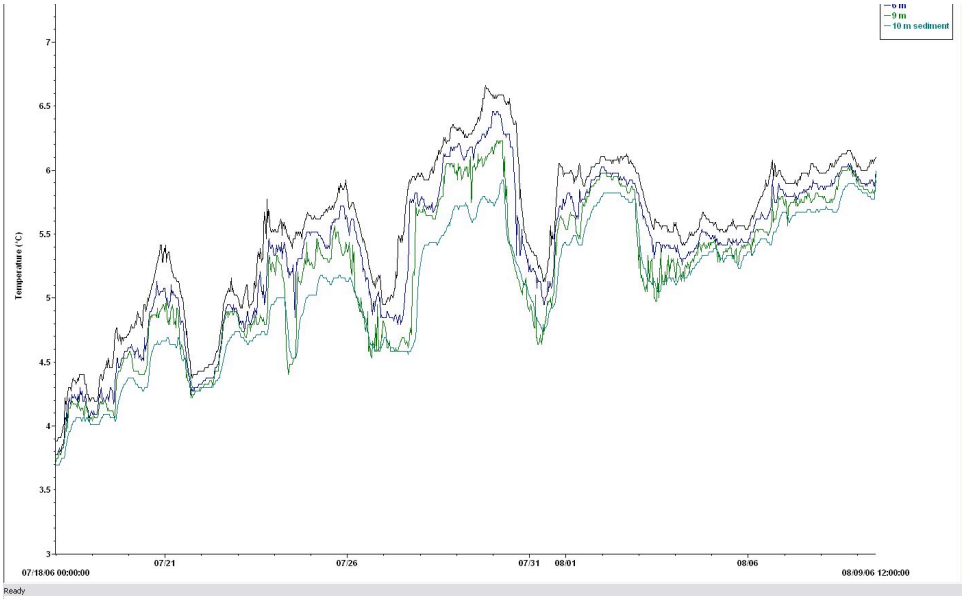

Figure 24. Water temperatures at mooring F from 18 July to 9 August 2006, at depths of 3 m, 6 m, 9 m, and the lake floor at 10 m.

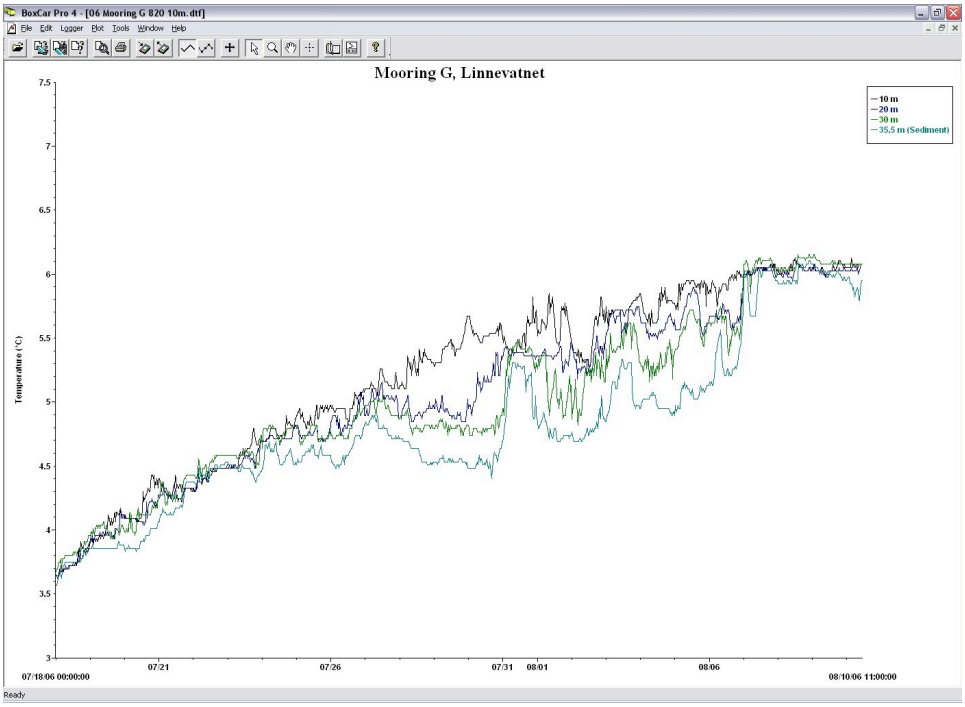

Figure 25. Water temperatures at mooring G from 18 July to 10 August 2006, at depths of 10 m, 20 m, 30 m, and 35 m.

3.2.1 Lake Temperatures and Meteorological Conditions

An attempt was made to find correlations between meteorological conditions and lake stratification behaviors. Due to time and space limitations of this paper, only mooring C, the mooring closest to the lake inlet, will be compared to each recorded meteorological factor. Wind direction appeared to have the greatest influence on the lake temperatures at depth. When the polar northeasterly winds blew over the lake, there was a significant decrease in lake temperatures in the first few meters depth (Figure 26). There also appeared to be a slight relationship between wind velocity and mooring C lake temperatures (Figure 27). No strong correlation was found between mooring C lake temperature and the air temperature (Figure 28). Similarly, precipitation did not affect lake temperatures (Figure 29). Lastly, no strong correlations could be found between mooring C lake temperatures and solar radiation in Linnédalen (Figure 30).

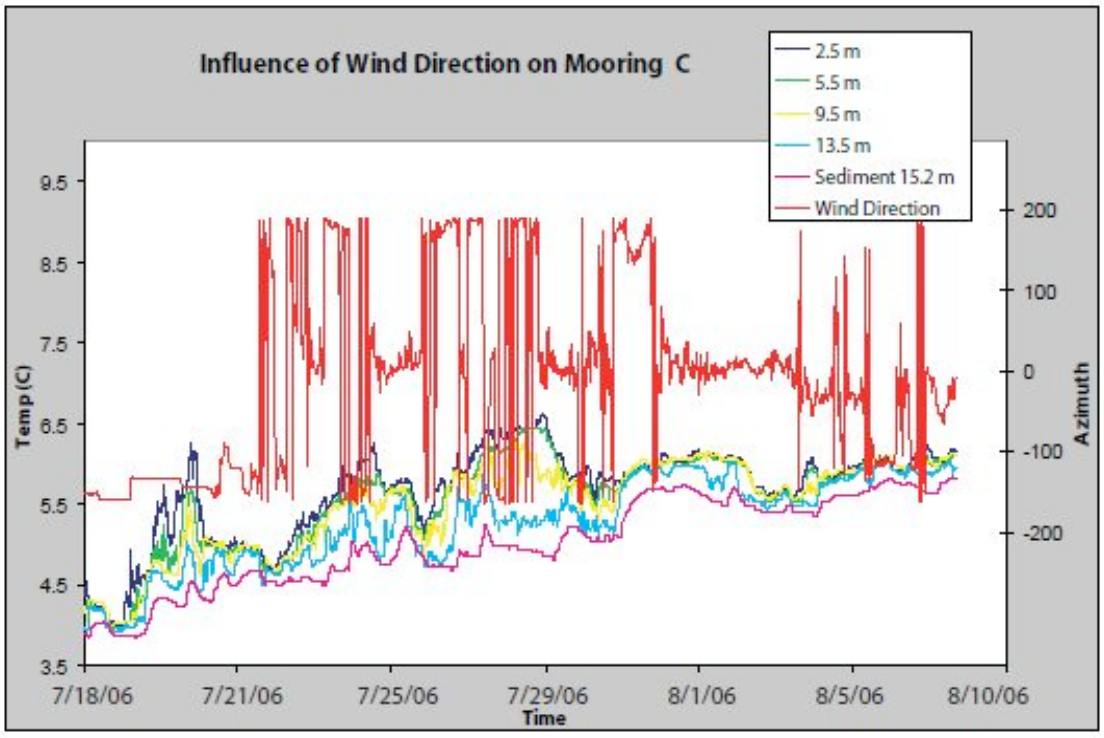

Figure 26. Wind direction and mooring C water temperatures from 18 July to 10 August 2006. Polar winds decrease lake temperatures.

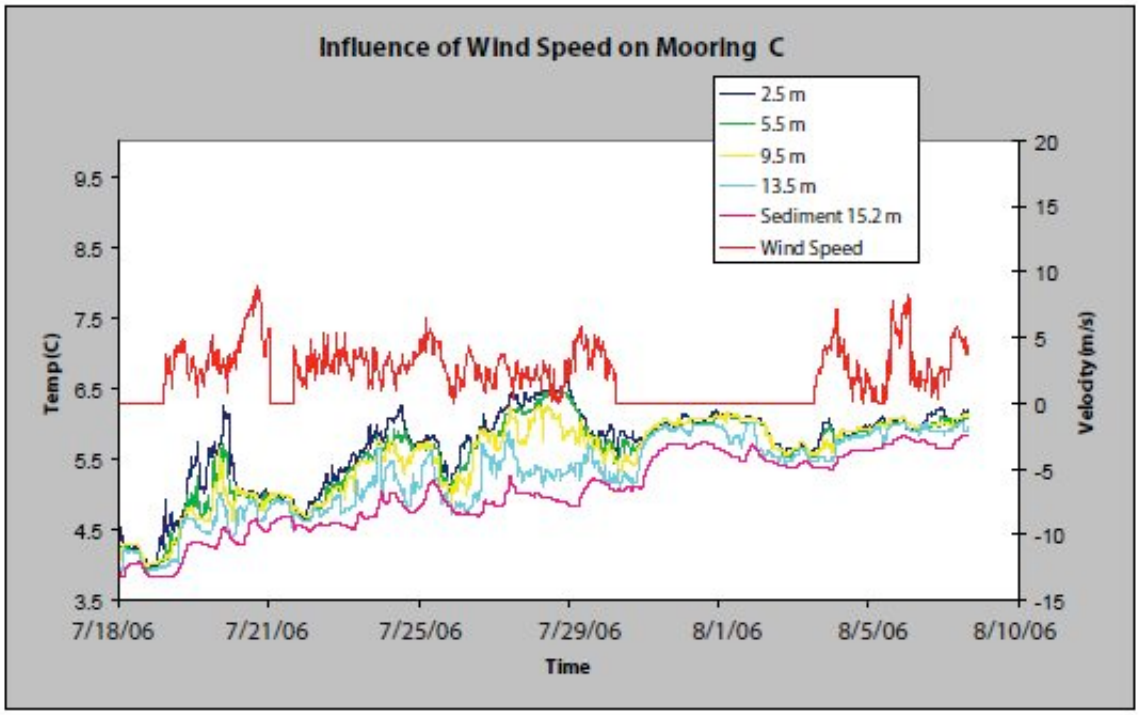

Figure 27. Wind speed and mooring C water temperatures from 18 July to 10 August 2006. Sometimes mixing occurs after higher wind speeds.

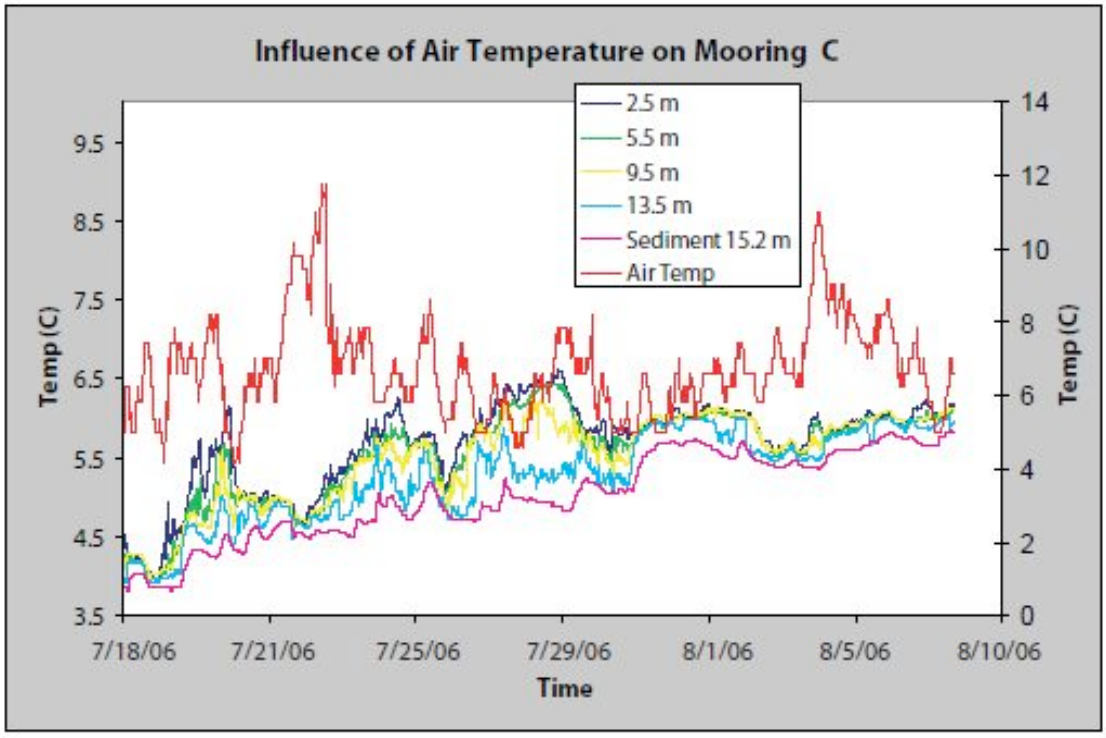

Figure 28. Air temperature and mooring C water temperatures from 18 July to 10 August 2006. There are no apparent correlations.

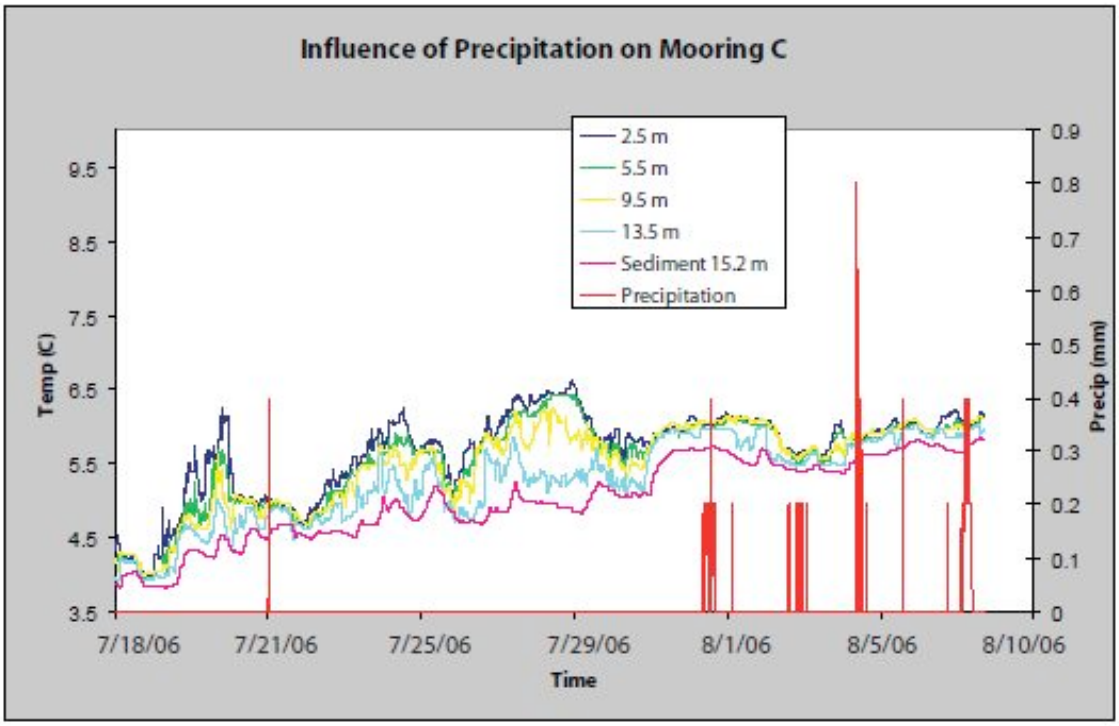

Figure 29. Precipitation and mooring C lake temperatures from 18 July to 10 August 2006. There are no apparent correlations.

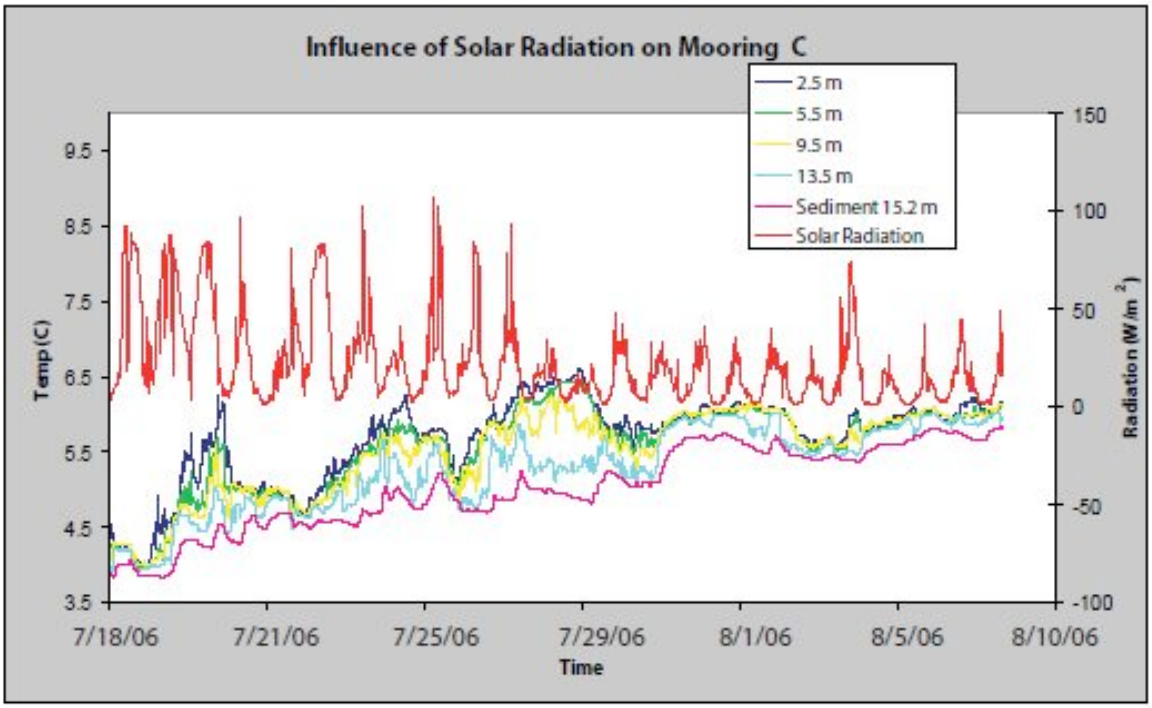

Figure 30. Solar radiation and mooring C lake temperatures from 18 July to 10 August 2006. There are no apparent correlations.

3.3 Water Column Profiles

Ninety-four water profiles were recorded from Linnévatnet. These vertical water casts reveal intermittent stratifications in transmissivity. Stratifications of lower percent light transmission indicate the presence of density currents including overflows, interflows, underflows, as well as turbidity currents.

Relative decreases in transmissivity at the top of water columns were observed in Linnévatnet. These sediment plume overflows were the most common type of density current entering the lake from Linnéelva; they were visible each day. The percent light transmission in these overflows varied greatly, as did their extents. At the lake inlet, overflow transmissivities ranged from 20 percent to 50 percent light transmission while

the mean transmissivity of the ambient water was 61 percent light transmission. At mooring C, away from the lake inlet, overflow transmissivities ranged from 40 percent to 50 percent. Figure 31 shows the vertical transmissivity profile for an overflow current at mooring C, located in front of the lake inlet. The water column profiles did not detect overflows at moorings D, E, F, and G. Vertical casts intermediate to the five mooring sites allowed for recording density currents at a higher resolution to track the currents through the lake at a range of depths.

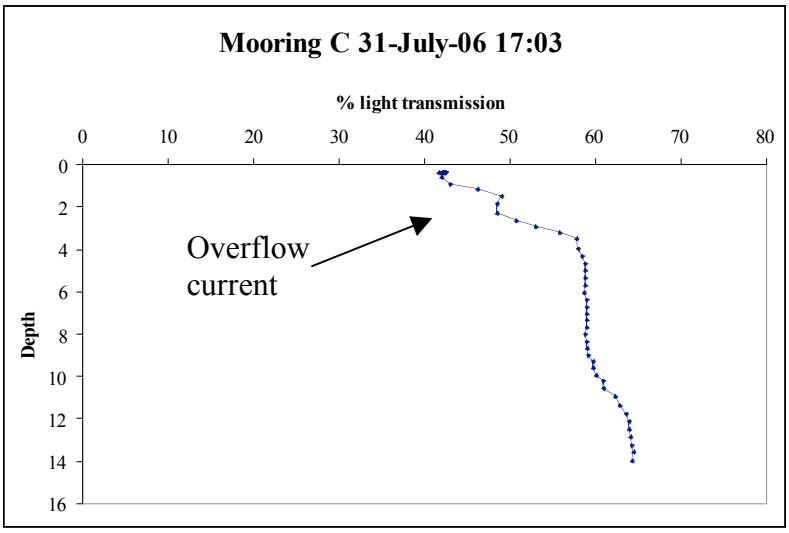

Figure 31. Vertical transmissivity profile for an overflow current at Mooring C.

Underflows were the second most common type of density current observed in the lake. No underflows were observed directly at the lake mouth. Underflows were detected throughout the field season. The underflows seemed to be detected in the eastern half of the lake, consistent with the direction of the lake inflow. Halfway between the red boat mooring (75 m out from the inlet) and the east shore, underflows were detected on 29 July at 15:21, and on 1 August at 11:46. Figure 32 shows the transmissivity profile of the underflow on 1 August. On 3 August 11:58 an underflow

current was isolated at the red boat mooring and mooring C; the turbid water of the underflow current were not detected in intermediate water column casts at the inlet and at mooring D. Similarly, on 13 August 16:01 to 16:55 the extents of underflow currents were constrained at mooring sites by Seacat casts. At mooring G, north of the Island, there were transmissivities of 59% light transmission in an ambient lake transmissivity of 76% light transmission. This same underflow was followed back to mooring D, and mooring C. The turbidity current ceased between mooring C and the red boat mooring. Figure 33 shows water column profiles of the red boat mooring and half way between mooring C and the red boat mooring illustrating the cutoff of an underflow current. Water column profiles detected transmissivities at mooring C ranging from 8 to 38 percent light transmission, with an average of 22 percent. The ambient lake transmissivities at these times ranged from 62 to 72 percent, with an average of 68 percent.

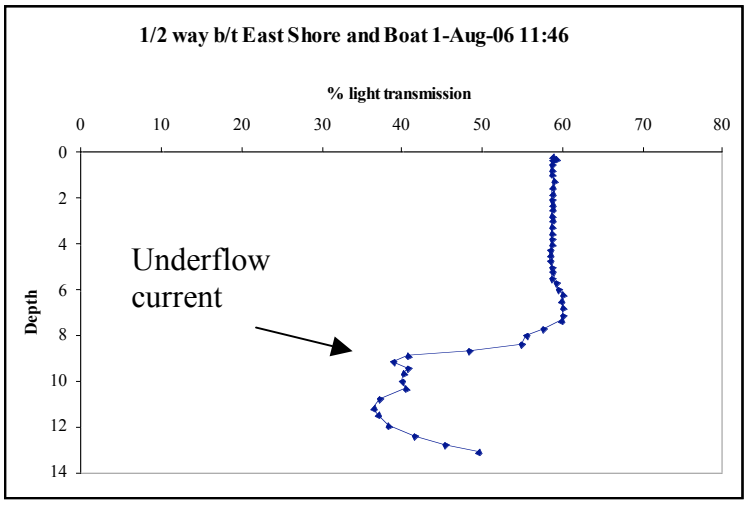

Figure 32. An underflow current half way between the east shore and the red boat.

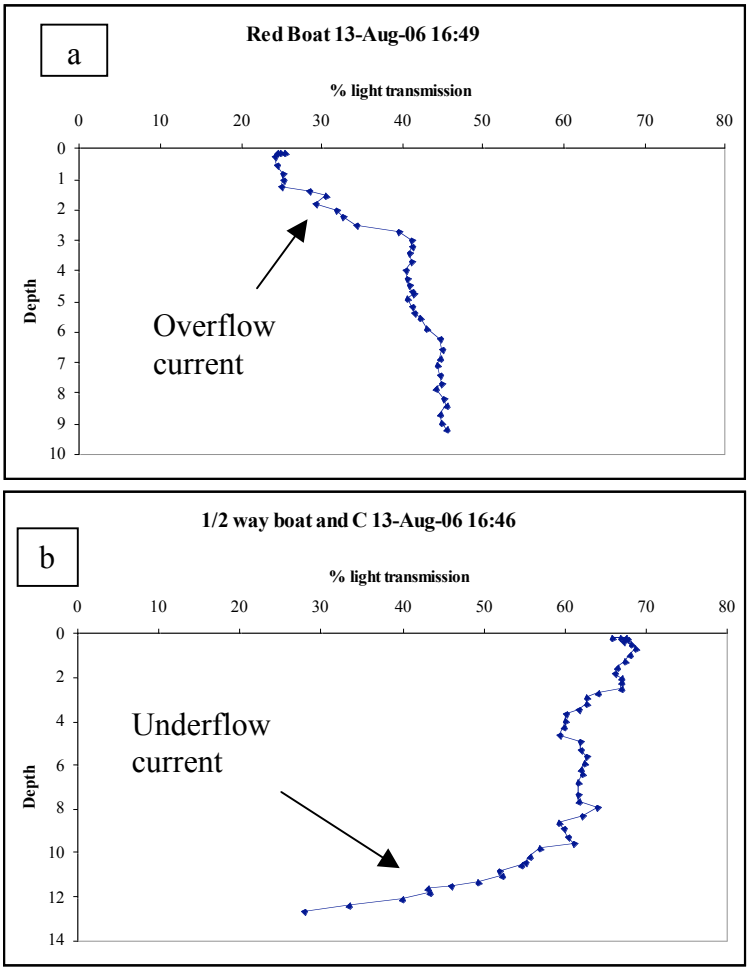

Figure 33. The transmissivities from the red boat (a) and half way between the red boat and mooring C (b) reveal the termination of an overflow and beginning of an underflow current. The red boat and mooring C are only about 100 m apart from each other.

Only one vertical cast revealed a density current in an intermediate water column depth segment, potentially suggesting an interflow current. This interflow of 44% transmissivity was captured at mooring C at 11:42 on 30 July (Figure 34). At this same time, an overflow extended out from the lake inlet, with no detection of interflows closer towards the inlet.

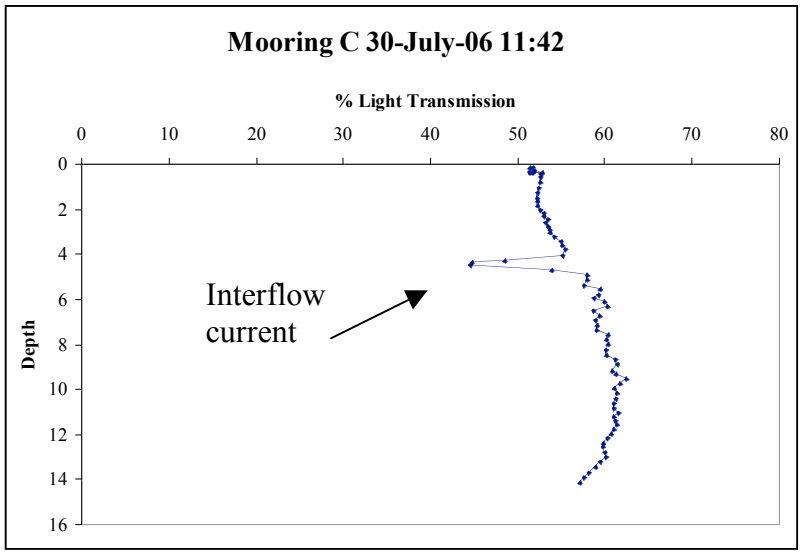

Figure 34. The transmissivity profile of the only interflow detected within Linnévatnet.

Underflows interpreted to be delta turbidity currents were detected twice. These currents were always abrupt in the water column, had thicknesses of two meters or less, and had significantly higher deviations in transmissivity from the ambient lake water than any other density flows (Figure 35). Delta turbidity currents were likely a result of delta front slope failures. The delta front continuously receives an accumulation of new sediment, which over-steepens the delta slope. Delta front failures result in bottom turbidity flows. Failures of the delta front are not particularly related to local meteorological conditions, but rather, the slow continuous deposition of unstable sediment.

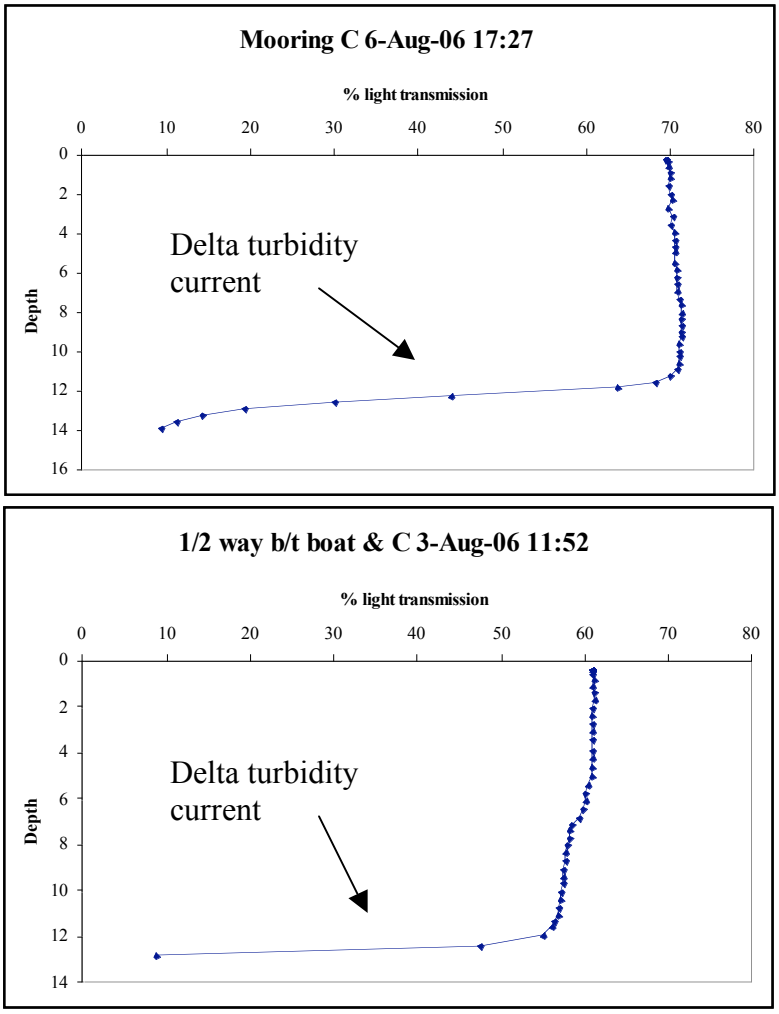

Figure 35. Great increases in turbidity in the bottom meter of the water column probably are the result of delta turbidity currents.

It is important to note that there were periods when the transmissivity contrast was not great enough to detect individual flows in the water column, suggesting homopycnal currents as a result of relatively uniform water density. Figure 36a shows a cast taken at the red boat mooring on 5 August 2006 which indicates a homopycnal flow in the water column; the observed transmissivities of this cast are much less than the typical ambient lake transmissivity. Similarly, Figure 36b shows a water column cast with no discernable stratified turbidity flow, yet the transmissivities were lower than the

normal ambient lake transmissivities, indicating a complete mixing of the water columns at this particular mooring site.

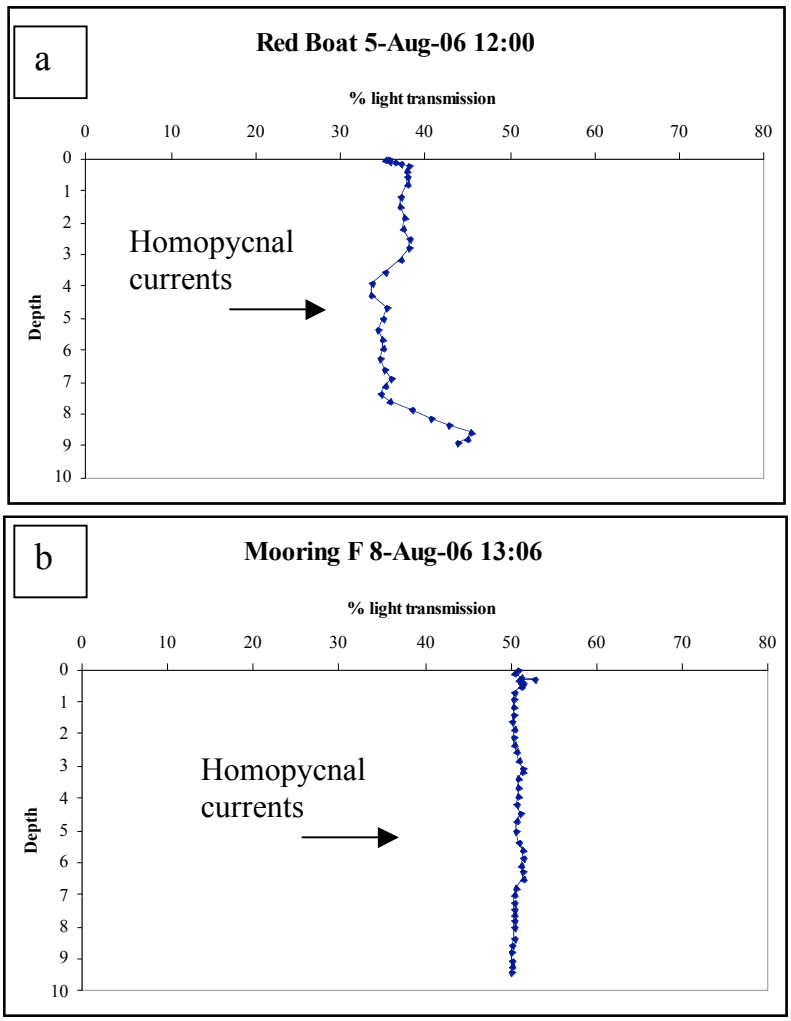

Figure 36. Homopycnal currents in Linnévatnet, as a result of mixing from wind and wave action. These currents have fluctuating transmissivities (a) and uniform transmissivities (b) in the water column, but are still below the normal ambient lake transmissivity.

3.4 Correlating Lake Density Currents and Meteorological Conditions

No single meteorological factor could be categorized as the principal agent in the Linnévatnet system. While there is a link between Linnébreen glacier ablation, discharge, and water densities of sediment-laden meltwater, the Linné valley spans 15 km in length (including the 4.7-km-long lake); the valley acts as both a sediment sink and source, and is greatly influenced of meteorological conditions.

Despite the absence of a single principal factor in the Linnévatnet system, there were several agents which affected the breadths and depths of density currents. First, wind was a dominant influence on not just the lake inlet, but the entire fetch. In the first few meters depth at the lake inlet, the turbidity decreases with the absence of wind between 1August to 6 August (Figure 37). This same phenomena occurred more distal from the lake inlet, in the first few meters depth at mooring C (Figure 38). In addition to the wind, precipitation and air temperature seemed to have an influence on lake turbidity currents. On 6 August and 7 August, there was a spike in air temperature followed by an intense precipitation event. These two events coincided with a rapid increase in turbidity in the upper 4 m of the lake inlet, and an increase in turbidity at all depths at mooring C. Below 4 m at the lake inlet, there was no transmissivity increase, however on the lake bed at mooring C, a significant underflow occurred with less than 20% light transmission, possibly from a deltaic density current triggered by failure of unconsolidated delta deposits; it was not detected 1 m above the lake bottom. Precipitation may have also played a role in a transmissivity increase visible at 12 m and 13 m depths, on 4 August. There are no other apparent meteorological agents that seemed to relate with these transmissivity spikes.

There were turbid density currents that had no apparent meteorological influence. For example, at 2 m, 4 m, and 6 m depth at the lake inlet on 30 August, there are turbidity peaks that do not correlate with any meteorological condition. These may be a result of delta front failures. In all cases of density currents within Linnévatnet, solar radiation did not have any correlative relationships.

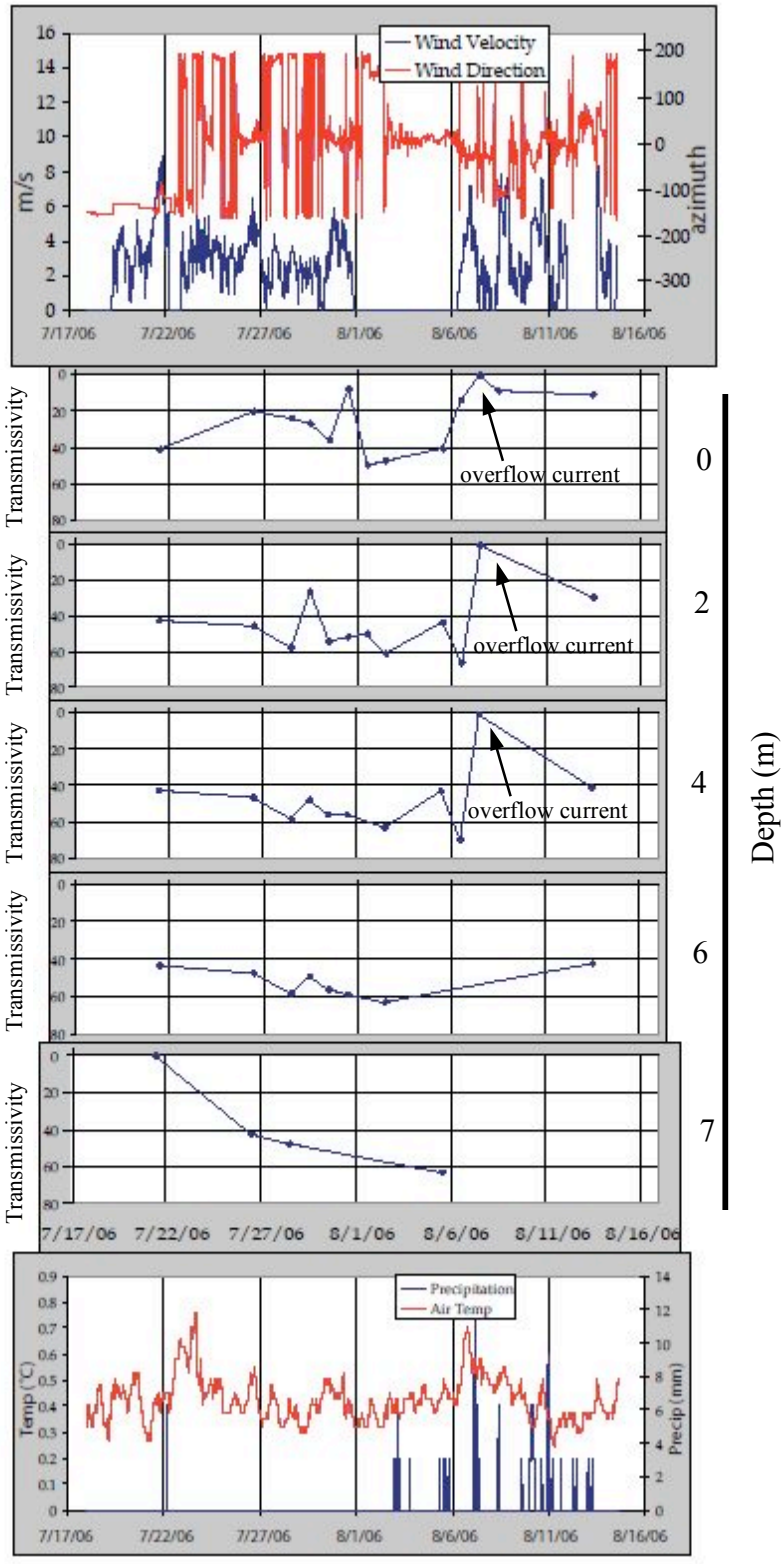

Figure 37. The influence of meteorological factors on lake inlet transmissivities at different depths from 17 July to 16 August 2006. Wind direction, air temperature, and precipitation may influence density flows. Note the overflow current on about 7 August.

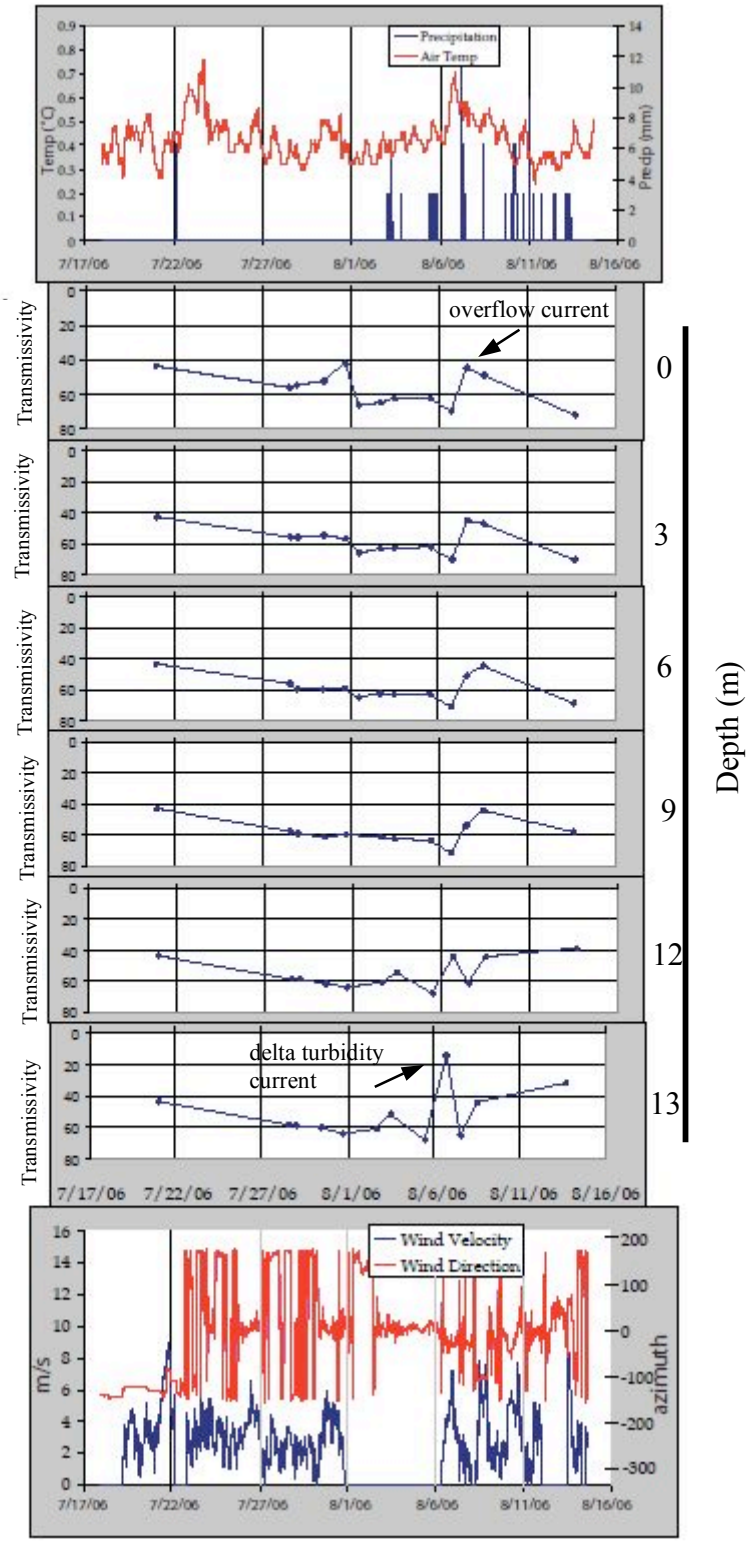

Figure 38. The influence of meteorological factors on mooring C transmissivities at different depths from 17 July to 16 August 2006. Wind direction, air temperature, and precipitation may influence density flows. Note the delta turbidity current and the overflows.

3.5 Water Temperature and Density Currents

There are intermittent correlations between lake temperatures and turbid density currents. For example, on 29 July 2006, a temperature stratification of 0.2ºC corresponded with a turbidity stratification of about 22% light transmission differential (Figure 39). However, on 28 July 2006, there was a 0.7ºC temperature stratification, and no coincident stratification in transmissivity (Figure 40). There were also transmissivity stratifications and no coincident temperature stratifications. On 5 August 2006, lake temperatures at the inlet had a range of only 0.1ºC, although the transmissivity of the water column varied from 10% light transmission to 60% light transmission (Figure 41).

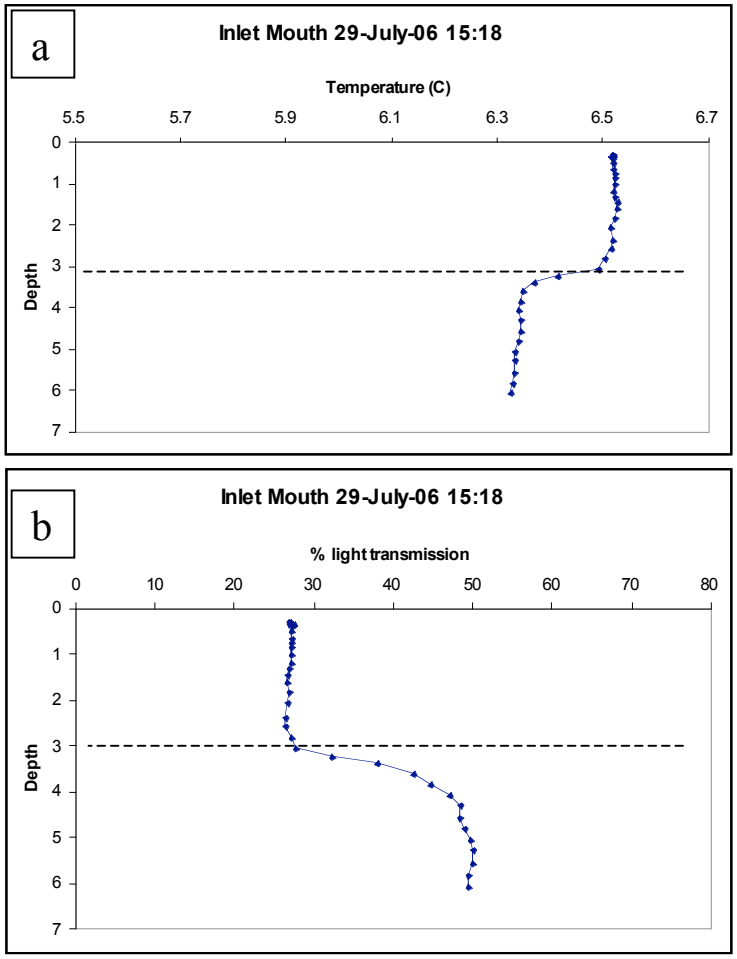

Figure 39. An apparent correlation between lake temperature (a) and transmissivity (b).

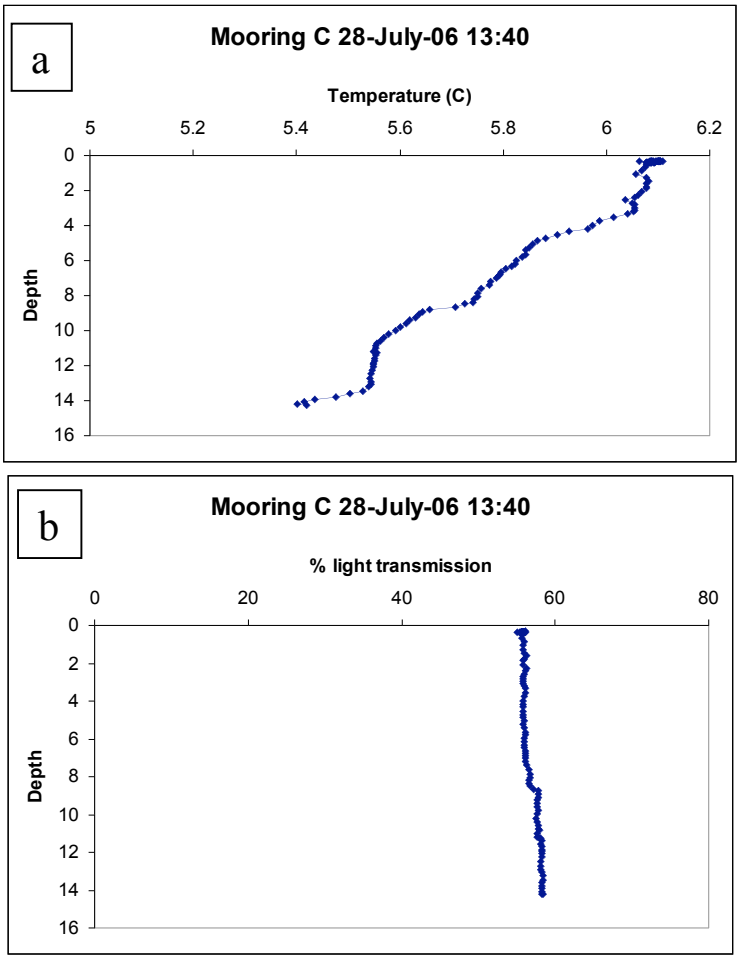

Figure 40. Variation in lake temperature (a), but no variation in transmissivity (b).

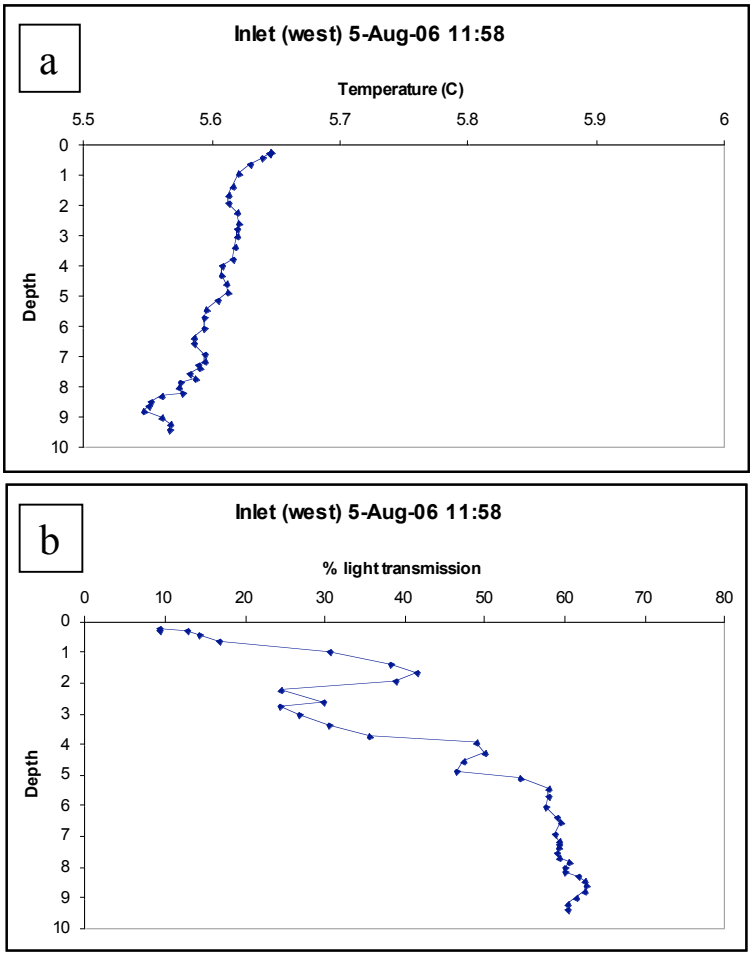

Figure 41. Little variation in temperature (a), but great variation in transmisivity (b).

3.6 Correlating Lake Inlet Currents and Suspended Sediment Concentrations

Discharge (Q) and suspended sediment concentrations (SSC) of July and August 2006 were calculated by Carr (2006) (Figure 42). There are relationships among turbid density currents, and Q and SSC, though the relationships are not strong enough to provide a definite correlation. On 6 August 2006, there was a spike in Q as well as SSC. This spike was seen in the upper 4 m at the lake inlet, though it did not show up in the bottom quarter of the water column (Figure 43). Out from the lake inlet, the surge in Q and SSC on 6 August 2006, as well as the succeeding turbidity increases, were detected

at all depths at mooring C (Figure 44). Interestingly, underflows at C traveled faster than the overflows. The underflows at 12 m and 13 m depth had a delay of less than 22 hours after the surge in Q and SSC, while the density currents in the upper portions of the water column (surface to 9 m) had a greater lag of approximately 43 hrs.

The discharge of Linnéelva is surely related to ablation rates and meteorological condition of the Linné valley, however, as previously stated, no single meteorological conditions could be pinned as the most influential or having the greatest effect on overflow, interflow, and underflow currents within lake Linnévatnet.

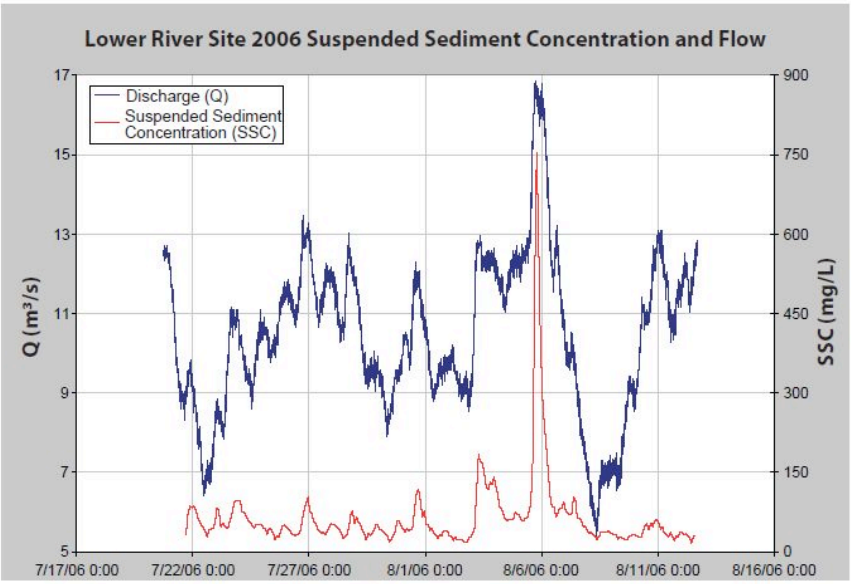

Figure 42. Suspended sediment concentration (SSC) and discharge (Q) of Linnéelva from 17 July to 16 August 2006. From Carr (2006).

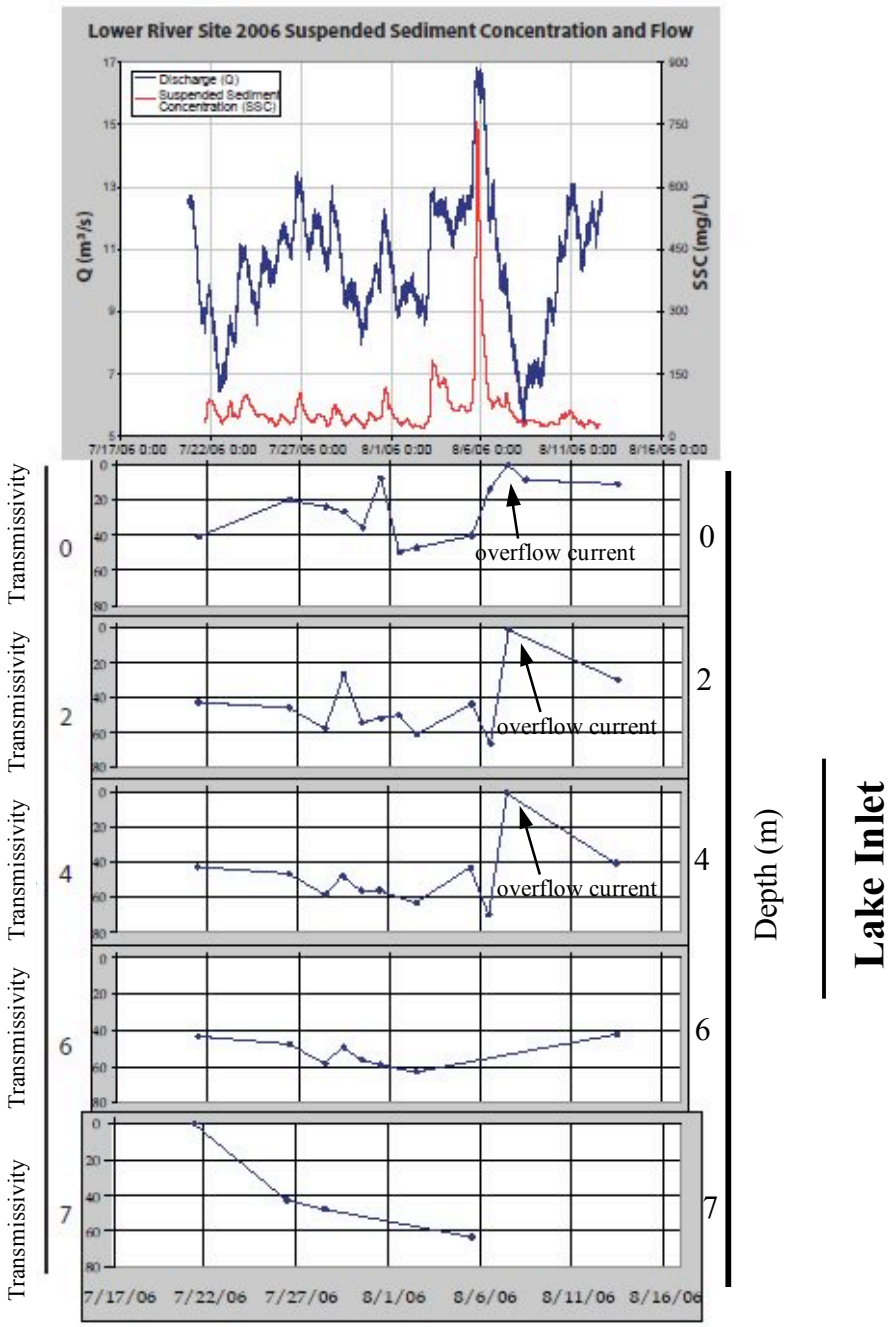

Figure 43. Discharge (Q) and suspended sediment concentration (SSC) compared with inlet transmissivities at different depths from 17 July to 16 August 2006. Notice relationship on 6 August between Q/SSC spike and overflow currents, though this relationship is not visible previous to 6 August.

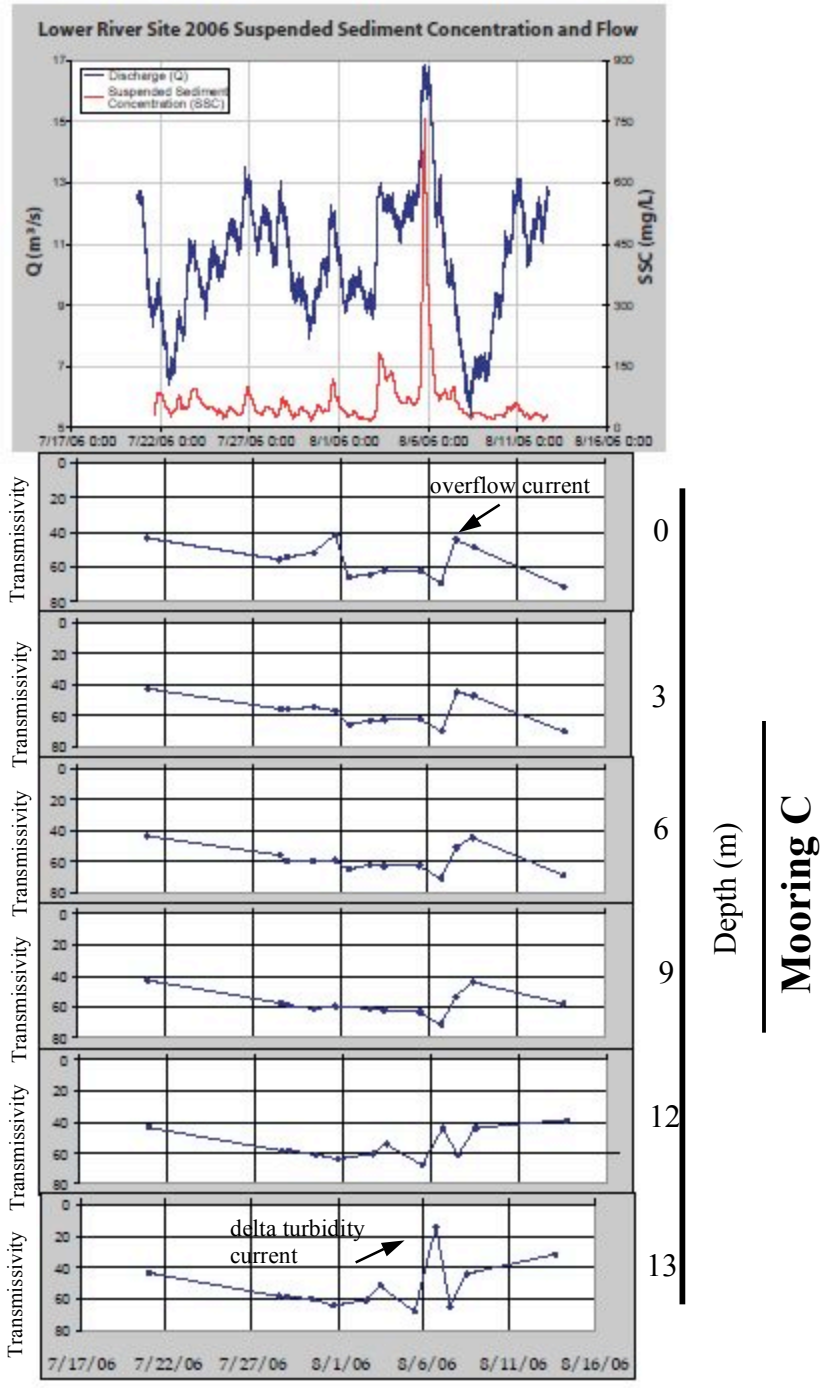

Figure 44. Discharge (Q) and suspended sediment concentrations (SSC) compared with mooring C transmissivities at different depths from 17 July to 16 August 2006. Notice relationship between Q/SSC spike and delta turbidity current, and slightly lagged overflow current.

3.7 Automated Remote Imaging

The automated remote camera captured 140 images of the south end of Linnévatnet from 22 July to 14 August 2006. The images reveal weather conditions, wave conditions on the lake, and surface sediment plume extents. The sediment plumes are enhanced with dotted lines in the accompanying figures. There are a few images that are not useful due to precipitation sprayed on the outer window of the camera. The camera images serve as an accompanying data set to visually represent the many factors influencing the Linnévatnet inlet regime. In a sense, these images combine all real-time data sources into one view.

The area of the surface sediment plume near the Linnévatnet inlet varied greatly. While each image provides a wealth of information, this paragraph will highlight a few plume events characteristic of the entire field season. Overflow turbidity currents generally migrated in a counter-clockwise fashion, as a result of the northeast direction of lake inflow, as well as slight influence of the Coriolis effect. Figure 45 illustrates an individual migration of a surface overflow plume. On 1 August 2006, overflow plumes dominant on the eastern slope (8:15) became accompanied by an overflow plume more proximal to the lake inlet (11:15), stretching out toward the center of the lake. Three hours later (at 14:15), the overflow retreated, forming cut-off plumes proximal to the source. According to Carr (2006) who observed and recorded the river conditions during this field season, the discharge increased between 8:15 and 11:15, though the suspended sediment concentration decreased. Between 11:15 and 14:15 the discharge decreased and the suspended sediment concentration was even lower than before, thus forming the cut-

off plumes. Additionally, the northerly winds were dominant at 8:15, while there was no wind activity at 11:15 and 14:15.

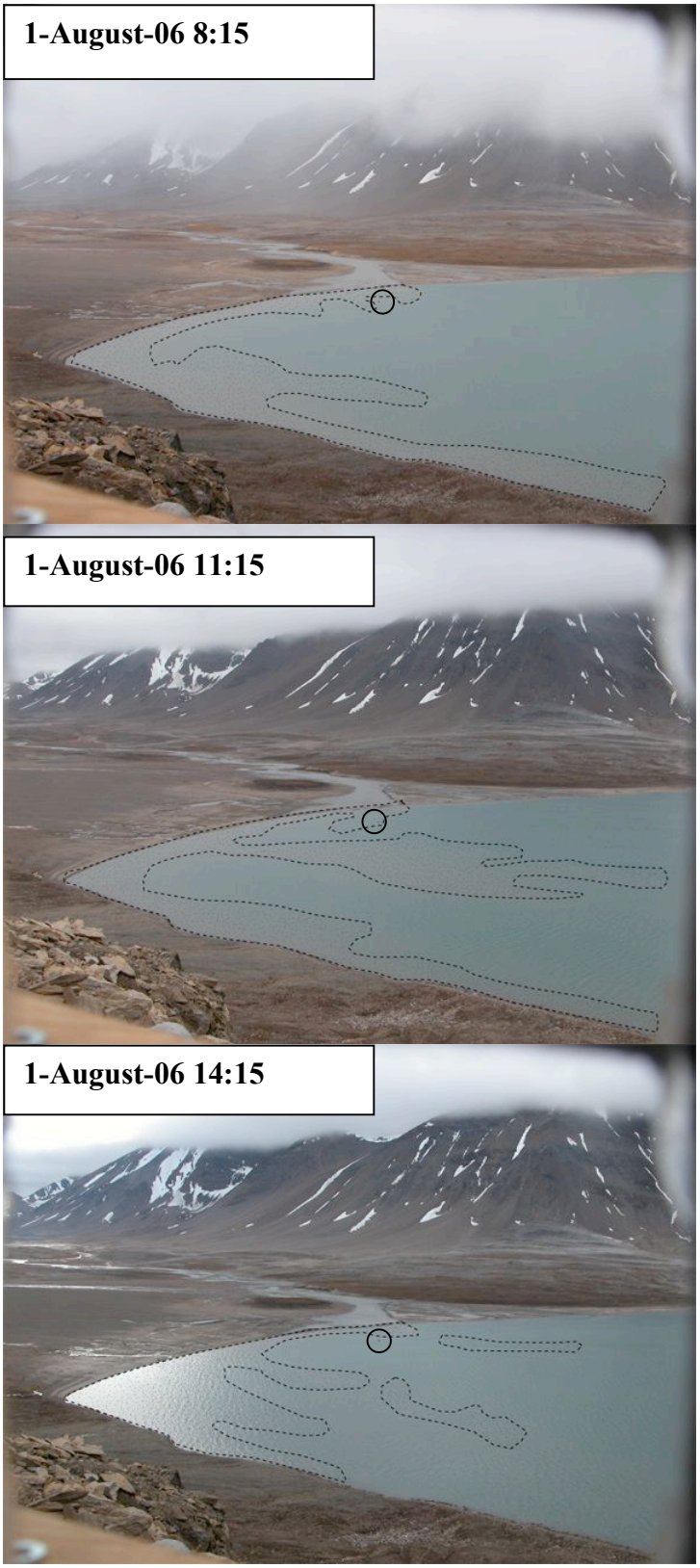

Figure 45. Surface sediment plume progression. In just three hours, an overflow turbidity current changes shape and extent. Sediment plumes outlined. Row boat in circle for scale. View southwest.

The influence of wind on the surface sediment plumes was very apparent from automated camera images. Figure 46 shows images captured on 28 July 2006 at 2:15 and 5:15. The 2:15 image shows the overflow sediment plume moving in a counterclockwise fashion, while the 5:15 image shows a linear, more stretched out pattern of the sediment plume. In the three hours between the two images, the discharge decreased, the air temperature decreased, there was no precipitation, and the wind blew from the south between 2 m/s and 3 m/s. A more stretched out plume from the south end of Linnévatnet, the presence of southerly winds, and notably the decrease in stream discharge, suggests that it was predominantly winds that transferred the lake surface plume northward.

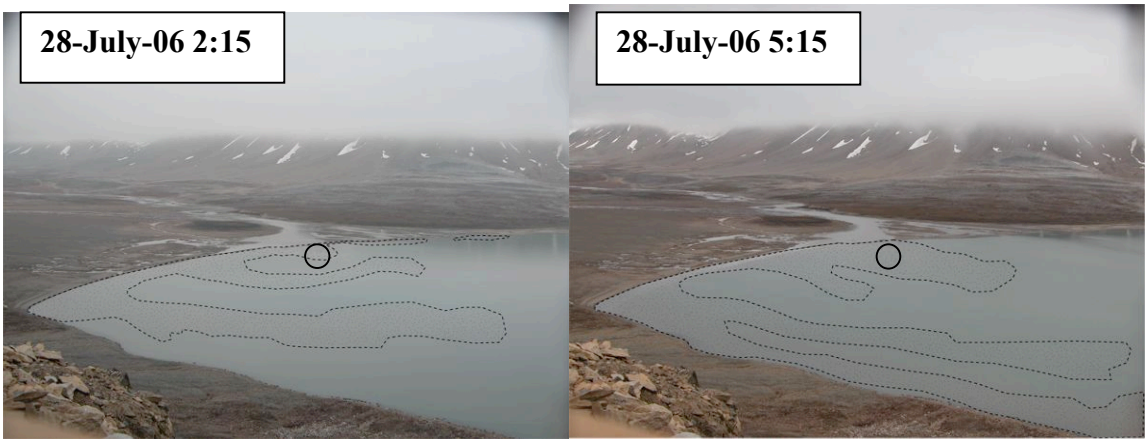

Figure 46. The elongation of surface sediment plumes. Sediment plumes outlined. Row boat in circle for scale. View southwest.

Likewise, in addition to low stream discharge, polar northeastly winds inhibited overflow currents in the lake. The automated camera captured periods without broad overflow sediment plumes (Figure 47). On 8 August 2006 at 17:15, and three hours later at 20:15, the Linnéelva discharge was low (Carr, 2006). Additionally, the wind was blowing from the northeast, as seen by reduced wave height along the east coast. The wind was effectively blocking the extent of the overflow plume, however the mixing within the water column at these times increased due to increased turbulence.

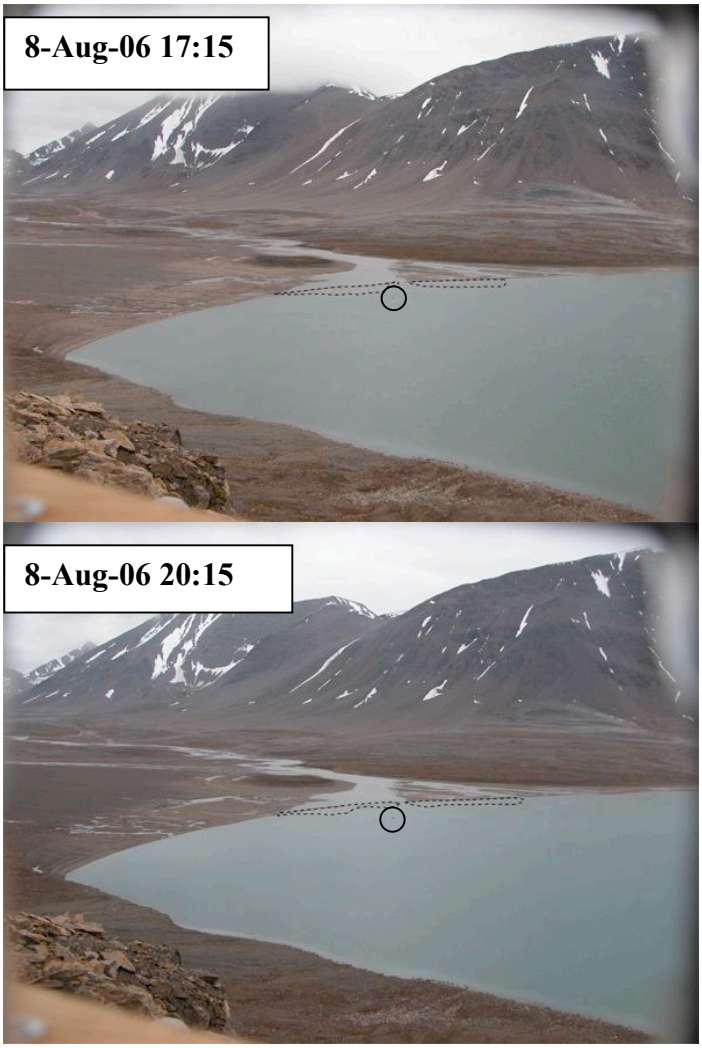

Figure 47. Minimal extent of sediment plumes (outlined) coinciding with northerly winds. Row boat in circle for scale. View southwest.

4. Discussion

4.1 Discharge and Suspended Sediment Concentration

The Linné valley acts as both a sediment sink and sediment source. In the summer months, most grains sand-sized and larger are deposited before entering Linnévatnet, however during times of high discharge, the once-deposited sediment becomes remobilized in the braided stream and advances toward the lake. Sediment is continually mobilized and deposited as a result of varying discharge from spring to autumn. Matelle (2006) found that the suspended sediment load dropped by 80% as the stream passed through the Linné valley toward Linnévatnet. Most mobilization of sand and coarser grains occurs during the spring months when ice melts and discharge is at its peak, though in July and August, silts and clays are still suspended in the river entering Linnévatnet resulting in density flows extending through the water.

Carr (personal communication, 2007) attempted to find direct relationships between discharge (Q), suspended sediment concentrations (SSC) and meteorological factors, but no single factor could be directly linked. Additionally, besides meteorological conditions, glacier hydrology and denudation rates also influence Q and SSC. The focus of this paper is not on Q and SSC, but on the turbid density flows formed in lake Linnévatnet, and constraining their activity.

4.2 Linnévatnet Density Currents

Subaqueous density flow paths were traced by taking subaqueous water column profiles at set positions from the south end of Lake Linnévatnet to the inlet. Overflows were the most common type of density flow. This is likely due to the silt and clay grains

suspended at the river outlet. Linnéelva river travels approximately 5 km down-valley from Linnébreen, with changes in gradients along its path; most sand-sized and larger sediments are deposited before reaching Linnévatnet. The sediment overflows in Linnévatnet could not be directly linked to specific individual meteorological conditions, though interplays were found between wind direction, wind velocity, precipitation, air temperature, and overflow behavior. Camera images provide visual evidence for overflow plume variations and meteorological conditions.

We found underflows to be the most dominant form of density currents within Linnévatnet. Roop (2007) found similar signals of an underflow-dominant transportation regime at the southern end of the lake. Underflows indicate that the density of incoming water was greater than the density of the lake water. Because sediments were still entering the lake in mid August, considerably after the supposed nival melt pulse, the sediment depletion within the valley may be low. It is unknown as to whether there was a strong nival pulse of sediment with the spring melt, or if there is a constant suspended sediment concentration throughout the spring and summer. Lake sediment cores and sediment traps assist in answering this question.

Overflows were the principal density currents tens of meters proximal to the lake inlet. This may be a function of a horizontal discharge vector which keeps the sediments in suspension proximal to the inlet, but then velocity decreases, and the greater density of the sediments results in deposition distal to the lake inlet.

Of all the meteorological conditions recorded in the valley, wind was found to have the greatest influence on the density currents in the lake – not just in the uppermost water column, but also in the entire depth of Linnévatnet. For instance, when the wind

blew from the north on 8 August, it pushed the surface sediment plume back toward the lake inlet, while thoroughly mixing the water. The water column profiles of this mixed water revealed no overflows, no interflows, and no underflows, however the water transmissivities measured throughout the lake showed high turbidities (50% light transmission) relative to the normal ambient lake turbidity levels (normally between 60% and 70% light transmission) (ex. see figure 35). The uniformly-mixed water extended from the lake delta to beyond mooring F, 750 m away. After this event from the northerly winds, underflow currents became increasingly more abundant. As the northerly winds pushed the suspended sediments back toward the lake inlet, it is probable that the delta front deposits were disturbed, resulting in a vulnerability to delta failure turbidity currents. This could explain the presence of prominent underflow currents and delta turbidity currents after northerly wind events. When the wind blew from the south, there was a considerable difference in the behavior of the overflow currents as recorded by the automated camera. The presence of southerly winds elongated the overflow plumes away from the lake inlet. It is important to note that while the wind direction and velocity influences density currents, it is not the source of the currents; overflows were impelled by southerly winds, and restrained by northerly winds.

There were several incidences of homopycnal flows – episodes of turbid, unstratified mixing. Smith and Ashley (1985) believed that homopycnal flows are relatively uncommon in lakes fed by glacial meltwater. We believe that the homopycnal flows in Linnévatnet are not a result of equal densities between the river inflow and the lake water, but rather, a secondary result induced by meteorological conditions such as mixing by strong wave action during high wind velocities.

During the field season, only one single interflow density current was detected; overflows and underflows dominated the inflow regime. One potential reason for this may be the presence of two main active gyres within Linnévatnet (Figure 48). These gyres may originate from the kinematics of the river input and/or currents generated by wind at the lake surface. The density currents may preferentially occupy the upper or lower gyre currents. If such a flow regime exists, it may seasonal and only appear in the late summer. Roop (2007) deployed sediment traps at different depths at the southern end of the lake and did not detect interflows. Unfortunately there were no means to measure the velocity of the currents within the lake to substantiate the lake gyre model.

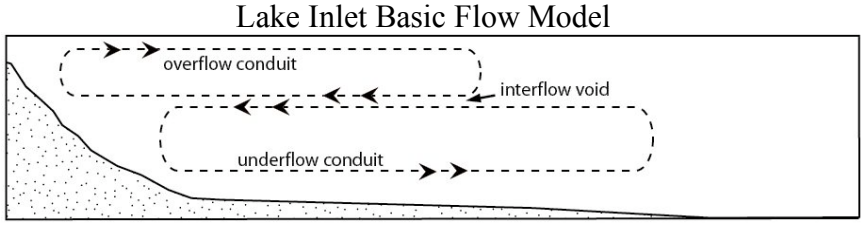

Figure 48. Cartoon of a proposed mechanism for obtaining overflow and underflow currents without intermediate interflow currents.

Helfrich (2007) found that mass wasting events on valley walls facing the Linné glacier accounted for most of the sediment concentration (SSC) increases detected approximately 1 km downstream. By 5 km farther downstream, most of these SSC pulses were severely attenuated or missing, except for the large spike on 6 August (see Figures 43, 44). The spike on 6 August was the result of a torrential precipitation event on the glacier on 5 August that triggered slope failures, increased SSC, and increased discharge (Q) (Helfrich, 2007). This meteorological event occurred only near the glacier; no precipitation occurred downvalley at the weather station near the lake. Underflows were present at the Linnévatnet delta after the increased SSC and Q. However, underflows were observed throughout Linnévatnet at times when there were no SSC and Q increases, suggesting influences beyond strictly meteorological conditions.

4.3 Lake Temperatures

Wind had an influence on lake temperatures. Winds blowing from the North Pole are considerably cooler than those blowing from the south west over the Gulf Stream. In the north-south trending Linné valley, polar northeasterlies decreased lake temperatures by as much as 1.5ºC (Figure 21). Lake temperatures during July and August 2006 ranged from 3.8ºC to 6.5ºC. Only one month earlier, June lake temperatures were still below 1ºC. Bøyum and Kjensmo (1978) believed that Linnévatnet was a cold meromictic (non-mixing) lake, experiencing temperatures of less than 4ºC all year, though this study shows that Linnévatnet reaches considerably warmer temperatures in the summer months. From mid October through May, however, the lake is completely frozen over.

The greatest density of water is at approximately 4º C, though there was no overturning or mixing in Linnévatnet as a result of crossing this temperature threshold. The lake was predominantly thermally stratified throughout July and August 2006 , although periodic mixing from abrupt cooling did disrupt the stratification. The mixing within Linnévatnet had a periodicity of approximately 4 days, which roughly coincided with the polar northerly wind events (Figures 21, 22, 23, 34). These cyclic mixing events were recorded in the mooring temperature loggers from 11 June, when the ice melted from the lake surface, to 11 August, the last day that the temperature loggers were in the water. The ultimate source of these cyclic mixing events is unknown.

4.4 Paleoclimatic Significance

Sediment cores are routinely used to interpret paleoclimates. Short sediment gravity cores were recovered from Linnévatnet during the summers of 2004, 2005, and 2006 in association with the Svalbard REU program. The cores revealed rhythmic silt and clay laminae at the submillimeter to millimeter scale (e.g.. Pratt et al., 2006; Werner et al., 2006). These laminae offer a detailed record of past weather and climate in the Linné valley, which is especially useful for detecting anthropogenic influences on the arctic climate.

The laminae of the Linnévatnet sediment cores are believed to be varves (e.g., Svendsen et al., 1989; Pratt et al., 2006; Werner et al., 2006). These probable varves must be interpreted with care. Results from this study indicate that sediments transported through Linnévatnet move in a roughly counter clockwise motion with highly variable paths. The turbidity currents within Linnévatnet are probably caused by local

meteorological conditions and delta front failures. As seen in the summer of 2006, just the direction of the wind can influence the extents of the sediment plumes within the lake. The wave-dominated delta at the south end of Linnévatnet indicates influential northerly winds and associated waves. Furthermore, fine suspended sediment loads within Linnéelva are subject to modification by meltwater from nearby snowfields. For example, meltwater from a small cirque approximately 800 m southwest of Linnévatnet introduced density currents other than those propagated by the Linné river. Because of the little transport distance to the lake, many of the density currents from this cirque meltwater were very turbid, with transmissivities as low as 5% light transmission. These turbid currents could deposit thick laminae during the melt season, which could potentially be mistaken as deposits from the main inlet river. As such, the lake sediment cores must not be misinterpreted, and multiple cores from various positions within the lake must be used to get the most accurate and representative record of past environmental conditions of the Linné valley.

The short sediment cores recovered in the summer REU programs came from moorings C, D, E, F, and G. During July and August, vertical water column casts showed that Mooring C had the most fluctuation between overflows and underflows, while only underflow turbidity currents were present at mooring D, E, F, and G. Thus, mooring D, E, F, and G may have significantly different sedimentology than closer to the lake inlet, such as at mooring C.

4.5 Other Sources of Sediment Input

Another source of sediment into the lake is by the migration of gelifluction lobes on the western and northwestern shores of Linnévatnet (Figure 49). These may introduce false climatic signals into the sediments recovered in lake cores. The lobes travel at a much slower rate than the river sediment input, and they are only active from spring to early fall when temperatures are above freezing, but they do flow to lake level. Waves up to 1 m high could easily assist the sediment transport from gelifluction lobes at the shore. Perreault (2006) found that increased clay deposition may be attributed to gelifluction input.

Figure 49. Gelifluction lobes on the western shore of Linnévatnet. Boulder in upper right is 30 cm across.

Disappearing streams are seen throughout the Linné valley. This may be a function of the permeability of the unconsolidated sediments of the piedmonts and braidplain. Additionally, the valley is underlain by discontinuous permafrost. Subsurface streams may be entering the lake during the summer months. While subsurface streams may not carry much sediment, they can potentially trigger turbidity flows.

4.6 Field Season Logistics and Early Summer Melt

Due to the nature of the National Science Foundation REU program, the field season took place in the summer. For logistical reasons, the program began 10 July and ended 15 August 2006. Without observing the turbidity currents in Linné earlier in the summer, it is unknown if the sedimentation processes we studied were a result of late-stage melting, or if the suspended sediment concentrations and transport that we observed were representative of the whole melt season. On 10 June, one month before arriving at Kapp Linné, there was still some ice present on the surface of the lake, as revealed by lake temperature loggers. Sediment transportation and deposition within Linnévatnet was surely influenced by this melting ice. When lake ice breaks up, it can redistribute shoreline materials, as well as rework littoral sediment by wave action (Woo, 1980; Doran, 1993). By studying sediment traps, Roop (2007) found that the sedimentation in Linnévatnet in the summer of 2006 was dominated by an early nival melt for a two-week period, and then was influenced mainly by the glacier meltwater system.

5. Conclusions

Lake Linnévatnet was dominated by overflows and underflows from mid-July to mid-August. The movement of these density currents was independent of grain size and water temperature; thus, interpreting lake density currents by grain size in sediment cores and by water temperature records, is risky in this High Arctic meltwater system. Furthermore, there were weak correlations between suspended sediment concentration (SSC), discharge (Q), and the occurrences and movements of the density currents within Linnévatnet. No strong, direct links were found between density currents and meteorological conditions, although relationships were observed between wind and near-surface sediment plumes. Polar northeasterly winds suppressed overflow sediment plumes and enhanced turbid underflows, while also increasing the chances of homopycnal flows. Southwesterly winds from over the Gulf Stream elongated surface sediment plumes. Density flows within the lake may be more closely related to delta front failure and mass wasting events upvalley near the Linnébreen glacier – at times, Linnébreen experienced much different meteorological conditions than down valley.

As a second objective of this thesis, lake temperatures were observed to characterize the summer thermal regime within Linnévatnet. Between June and August, surface lake waters warmed to nearly 7ºC, surpassing previously speculated maximum temperatures of 4ºC (Bøyum and Kjensmo, 1978). Lake temperatures were also strongly influenced by the wind.

Sediment cores recovered from Linnévatnet reveal rhythmic laminae of silts and clays, which may be used to understand the paleoclimate within the Linné valley. This study provides a better understanding of late summer sediment transport and deposition

in Linnévatnet, which in turn enables enhanced interpretations of the long-term Svalbard climate record.

5.1 Future Work

1) A full melt cycle study could provide a baseline context for the nival melt regime and sedimentation transport and deposition in Lake Linnévatnet from June through October rather than the limited three-week field season of this study.

2) Data from this study could be entered into Matlab for computational modeling and statistics such as time-series multiple linear regression tests. There are limited resources available at Whitman to run statistical analyses of the time series data set for the complex valley system. The components to correlate are: % light transmission of sediment plume, % light transmission of ambient lake, depth of water column and plume location therein, extent of sediment plume at each depth, lake temperature, air temperature, wind direction, wind velocity, precipitation, and solar radiation.

Acknowledgments

I would like to gratefully acknowledge the support of the National Science Foundation High Latitude Climate Change Science Program and the Svalbard REU program (NSF Award No. 0244097). A special thanks to the principle investigators and fearless trip leaders Al Werner, Mike Retelle, and Steve Roof. Additionally I would like to thank Mount Holyoke College and the University Centre on Svalbard (UNIS) for hosting the program. I am sincerely grateful to Bob Carson for his extraordinary guidance and his uncanny ability to teach by asking difficult questions. A big thanks to the 2006 REU participants Caroline Alden, Leif Anderson, Christina Carr, Eric Helfrich, Bennet Leon, Heidi Roop, and Heather Stewart, and a very special thanks to logistics expert Jørgen Haagensli of UNIS. Last but not least, I would like to gratefully acknowledge the support of Whitman College and my Geology and Environmental Studies colleagues.

Literature Cited

Adger, N., Aggarwal, P., Agrawala, S., Alcamo, J., Allali, A., Anisimov, O., Arnell, N., Boko, M., Canziani, O., Carter, T., Casassa, G., Confalonieri, U., Cruz, R.V., Alcaraz, E., Easterling, W., Field, C., Fischlin, A., Fitzharris, A., García, C.G., Hanson, C., Harasawa, H., Hennessy, K., Huq, S., Jones, R., Kajfez, L. Karoly, D., Klein, R., Kundzewicz, Z., Lal, M., Lasco, R., Love, G., Lu, X., Magrín, G., Mata, L.J., McLean, R., Menne, B., Midgley, G, Mimura, N., Mirza, M.Q., Moreno, J., Mortsch, L., Niang-Diop, I., Nicholls, R., Nováky, B., Nurse, L., Nyong, L., Oppenheimer, M., Palutikof, J., Parry, M., Patwardhan, A., Lankao, P.R., Rosenzweig, C. Schneider, S., Semenov, S., Smith, J., Stone, J., Ypersele, J.P., Vaughan, D., Vogel, C., Wilbanks, T., Wong, P.P., Wu, S., and Yohe, G., 2007, Intergovernmental Panel on Climate Change [IPCC]: Summary for Policy Makers.

Boggs, S., 2001, Principles of Sedimentology and Stratigraphy. New Jersey: Prentice Hall, 726 p.

Bøyum, A., and Kjensmo, J., 1978, Physiography of Lake Linnévatn, Western Spitsbergen. International Verein Limnology, 20, 609-614.

Carr, C., 2006, Suspended Sediment Transport in Proglacial Linnéelva, Spitsbergen. Earth Science Department B.Sc. Thesis: Montana State University, Bozeman, Montana.

Cohen, A, 2003, Paleolimnology: The History and Evolution of Lake Systems. Oxford University Press: New York.

Dallman, W.K., Hjelle, A., Andersen, A., Ohta, Y., and Salvigsen, O., 1992, Geological Map Svalbard 1:100,000. B9G Isfjorden: Oslo, Norsk Polarinstitutt, 52 p.

Doran, P.T., Wharton, R.A. Jr., and W.B. Lyons, 1994, Paleolimnology of the McMurdo Dry Valleys, Antarctica. Journal of Paleolimnology, 10, 85-114.

Gercke, E., 2006, Relationship Among Weather, Glacier Ablation, and Fluvial Processes, Svalbard, Norway. Department of Geology B.Sc. Thesis: College of William and Mary, Williamsburg, Virginia.

Giovanoli, F., 1990, Horizontal Transport and Sedimentation by Interflows and Turbidity Currents in Lake Geneva, *in* Tilzer, M.M. and Surruya, C. (eds.), Large Lakes: Ecological Structure and Function. Springer-Verlag, New York, 175-195.

Google Earth, 2005, Google Inc. Shareware.

Hardy, D.R., 1996, Climatic Influences on Streamflow and Sediment Flux into Lake C2, Northern Ellesmere Island, Canada: Journal of Paleolimnology, 16, 71-82.

Hodson, A., Gurunell, A., Tranter, M., Bogen, J., Hagan, J.O., and Clark, M., 1998, Suspended Sediment Yield and Transfer Processes in a Small High-Arctic Glacier Basin, Svalbard: Hydrological Processes, 12, 73-86.

Helfrich, E., 2007, Glacial Ablation Dynamics and Sediment Flux at Linnebreen, Spitsbergen. Department of Geology B.Sc. Thesis: University of Massachusetts, Amherst, Massachusetts.

Imboden, D.M. and Wüest, A., 1995, Mixing Mechanisms In Lakes, *in* Lerman, A., Imboden, D.M., and Gat. J. (eds.), Physics and Chemistry of Lakes, Springer-Verlag, New York, 83-138.

Ingólfsson, Ó., 2004, Outline of the Geography and Geology of Svalbard, Volume 2005: Longyearbyen, University of Norway in Svalbard (UNIS), UNIS course packet.

Johnsen, S.O., Mork, A., and Nagy, J., 2007, Outline of the Geology of Svalbard. Course material for Svalex Norwegian Universities Program.

Landvik, J.Y., Mangerud, J., and Salvigsen, O., 1987, The Late Weichselan and Holocene Shoreline Displacement on the West-Central Coast of Svalbard. Polar Research, 5, 29-44.

Lewis, T, 2000, Hydrometeorology and Lacustrine Sedimentary Processes at Bear Lake, Devon Island, Nunavut. Department of Geology Masters Thesis: Queen's University, Ontario, Canada.

Lewkowicz, A.G., and Wolfe, P.M., 1994, Sediment Transport in Hot Weather Creek, Ellesmere Island, Nwt, Canada, 1990-1991. Arctic and Alpine Research, 26, 213-226.

Maizels, J., 2002, Sediments and Landforms of Modern Proglacial Terrestrial Environments, *in* Menzies, J., Modern & Past Glacial Environments. Butterworth-Heinemann, Oxford, 279-315.

Marsh, P., and Woo, M., 1981, Snowmelt, Glacier Melt, and High Arctic Streamflow Regimes. Canadian Journal of Earth Sciences, 18, 1380-1384.

Mangrud, J., and Svendsen, J.I., 1990, Deglaciation Chronology Inferred from Marine Sediments in a Proglacial Lake Basin, Western Spitsbergen, Svalbard. Boreas, 19, 249-272.

Matell, N., 2006, The Role of the Valley Braidplain as a Sediment Sink: Linnédalen, Spitsbergen, Svalbard. Department of Geology B.Sc. Thesis: Williams College, Williamstown, Massachusetts.

McBean, G., Alekseev, G., Chen D., Foreland, E., Fyfe, J., Groisman, P., King, R., Melling, H., Vose, R., Whitfield, P., 2004, Arctic Climate Impact Assessment [ACIA]: Impacts of Warming Arctic. Cambridge: Cambridge University Press, 22-55.

Ohta, Y., Hjelle, A., Andersen, A., Dallmann, W.K., and Salvigsen, O., 1991, Geological Map of Isfjorden, Spitsbergen, Norsk Polarinstitutt Temarkart.

Overpeck, J., Hughen, K.A., Hardy, D., Bradley, R., Case, R., Douglas, M., Finney, B., Gajewski, K., Jacoby, G., Jennings, A., Lamoureax, S., Lasca, A., MacDonald, G., Moore, J., Retelle, M., Smith, S., Wolfe, A., and Zielinski, G., 1997, Arctic Environmental Change of the Last Four Centuries. Science, 278, 1251-1256.

Perreault, L.M., 2006, Mineralogical Analysis of Primary and Secondary Source Sediments to Linnévatnet, Spitsbergen, Svalbard. Department of Geology B.Sc. Thesis: Bates College, Lewiston, Maine.

Pickrill, R.A., and J. Irwin, 1983, Sedimentation in a Deep Glacier-fed Lake – Lake Tekapo, New Zealand. Sedimentology 30, 63-75.

Pratt, E., Werner, A., Roof, S., 2006, Characterization and Calibration of Lamination Stratigraphy of Cores Recovered from Lake Linné, Svalbard Norway. Abstract for 36th Annual International Arctic Workshop, Boulder, CO.

Retelle, M.J., and J.K. Child, 1996, Suspended Sediment Transport and Deposition in High Arctic Meromictic lake. Journal of Paleolimnology, 16, 151-167.

Richter-Menge, J., Overland, J., Proshutinsky, A., Romanovsky, V., Bengtsson, L., Brigham, L., Dyurgerov, M., Gascard, J.C., Gerland, S., Graversen, R., Haas, C., Karcher, M., Kuhry, P., Maslanik, J., Melling, H., Maslowski, W., Morison, J., Perovich, D., Przybylak, R., Rachold, V., Rigor, I., Shiklomanov, A., Stroeve, J., Walker, D., and Walsh J., 2006, State of the Arctic Report. NOAA OAR Special Report, NOAA/OAR/PMEL, Seattle, WA.

Roof, S., 2003, Linnévatnet Bathymetry and GPS Perimeter. Svalbard REU unpublished data.

Roop, H., 2007, Contemporary Lacustrine Sedimentation: Interpreting Inter and Intra-annual Sedimentation in Proglacial Linnévatnet, Spitsbergen, Norway. Department of Geology B.Sc. Thesis: Mt. Holyoke College, South Hadley, Massachusetts.

Schiff, K., 2004, Unsustainable Glacier Ablation at 78º N Latitude, Linnébreen, Svalbard. Department of Geological Sciences B.Sc. Thesis: Indiana University, Bloomington, Indiana.

Scholz, C.A., Jonson, T.C.. and McGill, J.W., 1993, Deltaic Sedimentation in a Rift Valley Lake: New Seismic Reflection Data from Lake Malawi (Nyasa), East Africa. Geology 21, 395-399.

Serreze, M.C., Walsh, J.E., Chapin III, F.S., Osterkamp, T., Dyurgerov, M., Romanovsky, V., Oechel, W.C., Morison, J., Zhang, T., and Barry, R.G., 2000, Observational Evidence of Recent Change in the Northern High-Latitude Environment: Climatic Change, 46, 159-207.

Smith, N.D., and G. Ashley, 1985, Proglacial Lacustrine Environment, *in* Ashley, G., Shaw, J., and Smith, N.D., eds., Glacial Sedimentary Environments. Soc. Econ. Paleo. Mineral. Short Course No. 16, 135-216.

Snyder, J.A., Werner, A., and Miller, G.H., 2000, Holocene Cirque Glacier Activity in Western Spitsbergen, Svalbard: Sediment Records from Proglacial Linnévatnet. Holocene, 10, 555-563.

Statistics Norway, 2005, Svalbard Statistics 2005. Official Statistics of Norway, D330.

Svendsen, J.I., and Mangerud, J., 1997, Holocene Glacial and Climatic Variations on Spitsbergen, Svalbard. Holocene, 7, 45-57.

Svendsen, J.I., Mangerud, J., and Miller, G.H., 1989, Denudation Rates in the Arctic Estimated from Lake Sediments on Spitsbergen, Svalbard. Paleogeography, Paleoclimatology, Paleoecology, 76, 153-168.

Watson, R.T., Albritton, D.L., Barker, T., Bashmakov, I.A., Canziani, O., Christ, R., Cubasch, U., Davidson, O., Gitay, H., Griggs, D., Halsnaes, K., Houghton, J., House, J., Kundzewicz, Z., Lal, M., Leary, N., Magadza, C., McCarthy, J.J., Mitchell, J.F., Moreira, J.R., Munasinghe, M., Noble, I., Pachauri, R., Pittock, B., Prather, M., Richels, R.G., Robinson, J.B., Sathaye, J., Schneider, S., Scholes, R., Stocker, T., Sundararaman, N., Swart, R., Taniguchi, T., and Zhou, D., 2001, An Assessment of the Intergovernmental Panel on Climate Change [IPCC]: Summary for Policymakers.

Werner, A., 1988, Holocene Glaciation and Climate Change, Spitsbergen, Svalbard. Department of Geological Sciences Ph.D. Dissertation: University of Colorado, Boulder, Colorado.

Werner, A., 1993, Holocene Moraine Chronology, Spitsbergen, Svalbard: Lichonometric Evidence for Multiple Neoglacial Advances in the Arctic. The Holocene, 3, 128-137.

Werner, A., Roof, S., and Retelle, M., 2006, Calibrating the Lamination Stratigraphy of Linné Valley, Svalbard, Noway: Research Results from the Svalbard REU Project. Abstract for 36th Annual International Arctic Workshop, Boulder, Colorado.

Wetzel, R.G., 1983, Limnology. Saunders College Publishing, Orlando, 767 p.

Woo, M., 1980, Hydrology of a Small Lake in the Canadian High Arctic. Arctic and Alpine Research, 12, 227-235.